

Lawrence Berkeley National Laboratory

Recent Work

Title

Vibrational Spectroscopy of the Ammoniated Ammonium Ions NH_4^+ (NH_3)_n (for n

Permalink

<https://escholarship.org/uc/item/8gd1k54k>

Journal

Journal of physical chemistry, 95(6)

Authors

Price, J.M.

Crofton, M.W.

Lee, Yuan T.

Publication Date

1990-05-01



Lawrence Berkeley Laboratory

UNIVERSITY OF CALIFORNIA

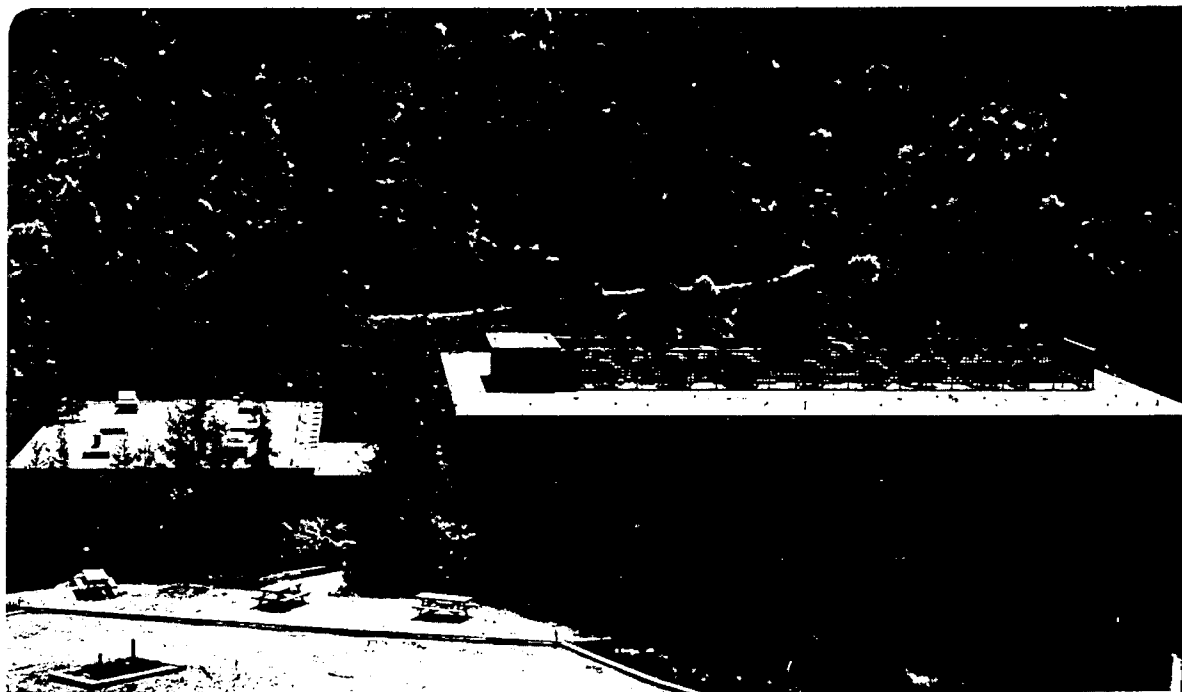
Materials & Chemical Sciences Division

Submitted to Journal of Physical Chemistry

Vibrational Spectroscopy of the Ammoniated Ammonium Ions $\text{NH}_4^+(\text{NH}_3)_n$ (for $n = 1-10$)

J.M. Price, M.W. Crofton, and Y.T. Lee

May 1990



LOAN COPY
Circulates
for 4 weeks

Bldg. 50
Library.

Copy 2

LBL-29016

DISCLAIMER

This document was prepared as an account of work sponsored by the United States Government. While this document is believed to contain correct information, neither the United States Government nor any agency thereof, nor the Regents of the University of California, nor any of their employees, makes any warranty, express or implied, or assumes any legal responsibility for the accuracy, completeness, or usefulness of any information, apparatus, product, or process disclosed, or represents that its use would not infringe privately owned rights. Reference herein to any specific commercial product, process, or service by its trade name, trademark, manufacturer, or otherwise, does not necessarily constitute or imply its endorsement, recommendation, or favoring by the United States Government or any agency thereof, or the Regents of the University of California. The views and opinions of authors expressed herein do not necessarily state or reflect those of the United States Government or any agency thereof or the Regents of the University of California.

Vibrational Spectroscopy of the
Ammoniated Ammonium Ions
 $\text{NH}_4^+(\text{NH}_3)_n$ (for $n = 1-10$)

J.M. Price, M.W. Crofton, and Y.T. Lee

Materials and Chemical Sciences Division
Lawrence Berkeley Laboratory
University of California
Berkeley, CA 94720

This work was supported by the Director, Office of Energy Research,
Office of Basic Energy Sciences, Division of Chemical Sciences, of
the U.S. Department of Energy under Contract No. DE-AC03-76SF00098.

Vibrational Spectroscopy of the
Ammoniated Ammonium Ions
 $\text{NH}_4^+(\text{NH}_3)_n$ (for $n= 1-10$)

J.M. Price, M.W. Crofton and Y.T. Lee

Materials and Chemical Sciences Division,
Lawrence Berkeley Laboratory and
Department of Chemistry, University of California,
Berkeley, CA 94720

ABSTRACT:

The gas phase vibration-internal rotation spectra of mass selected ammoniated ammonium ions $\text{NH}_4^+(\text{NH}_3)_n$ (for $n=1$ to 10) have been observed from 2600 cm^{-1} to 4000 cm^{-1} . The spectra show vibrational features that have been assigned to modes involving both the ion core species, NH_4^+ , and the first shell NH_3 solvent molecules. Nearly free internal rotation of the solvent molecules about their local C_3 axes in the first solvation shell has been observed in the smaller clusters ($n=1$ to 6). For the largest clusters studied ($n=7-10$) the spectra converge, with little difference between clusters differing by one solvent molecule. For these clusters, the spectrum in the $3200-3500 \text{ cm}^{-1}$ region is quite similar to that of liquid ammonia, and the entire region of $2600-3500 \text{ cm}^{-1}$ also bears considerable resemblance to the spectra of ammonium salts dissolved in liquid ammonia under some chemical conditions. This indicates the onset of a liquid-like environment for the ion core and first shell solvent molecules in clusters as small as $\text{NH}_4^+(\text{NH}_3)_8$.

INTRODUCTION:

Early spectroscopic studies of the ammonium ion were confined to the condensed phases and employed direct IR absorption measurements of either crystals of ammonium salts, or ammonium salts dissolved in solution.^{1,2,3} These measurements revealed spectral features that were assigned to vibrational modes of the perturbed NH_4^+ ion (T_d symmetry). Of these, the strongest in the 2000-4000 cm^{-1} region were found to involve the triply degenerate antisymmetric stretching motion ν_3 , and the first overtone of the doubly degenerate bending motion $2\nu_4$. (See fig. 1.)

Gas phase studies which followed, centered for the most part on the thermodynamics and kinetics of clustering reactions at relatively high pressures. Many investigators contributed in the effort to determine the ΔH^0 for formation of the solvated ammonium ion $\text{NH}_4^+(\text{NH}_3)_n$.^{4,5,6,7,8,9,10} Kebarle and coworkers showed that in the larger clusters there was a discontinuity in the ΔH^0 for the $n=4 \rightarrow n=5$ clustering step. This result was consistent with the idea that there were four solvent molecules involved in the first solvation shell of the cluster, with the solvent ammonias probably oriented along the N-H bonds of the ammonium ion due to ion-dipole interaction. A summary of these results appears in Table I, which lists the ΔH^0 of formation for each clustering step in the $\text{NH}_4^+(\text{NH}_3)_n + \text{NH}_3 = \text{NH}_4^+(\text{NH}_3)_{n+1}$ reaction series.

A fairly extensive body of theoretical work also exists, investigating the structure and thermodynamics of these systems. Pullman and Armbruster examined the thermodynamics of the stepwise

addition of H_2O or NH_3 to NH_4^+ for one to five solvent molecules and managed to reproduce the qualitative features of the experimental data.¹¹ The experimental change in preferential addition from NH_3 at low levels of solvation to H_2O at higher levels of solvation was reproduced. Errors in the energies calculated from the STO 3G basis set were found to decrease with increasing number of solvent molecules.

A more recent series of calculations on the thermodynamics of the $\text{NH}_4^+(\text{NH}_3)_n$ ($n=1-5$) ions as well as their detailed structures has been made by Hirao et al.¹² In this work, *ab initio* molecular orbital calculations determined the structure and binding energies of the series in reasonable agreement with high pressure equilibrium measurements. Values for the solvation energies obtained from this work, using 3-21G, 3-21G*, and 6-31G** basis sets yielded consistently higher values than experimentally obtained.

Gas phase spectroscopic measurements for the ammonium ion and the ammoniated ammonium clusters have only recently been carried out. The development of velocity modulation spectroscopy has yielded a great deal of information for a wide range of molecular ions, including the NH_4^+ ion.¹³ The ν_3 band of the ammonium ion has been investigated at high resolution by both Crofton and Oka¹⁴ and Schafer and Saykally¹⁵ using this technique. From this data an accurate equilibrium geometry has been obtained.¹⁴ Table II lists the measured rotational constants, and equilibrium geometry parameters for this ion and the NH_3 molecule. The only measurements of the spectra of the ammoniated ammonium ions ($n=1$ to 4)

have been limited to the direct absorption measurements performed by Schwarz in 1980 in a pulsed radiolysis of a gas cell containing ammonia in a helium carrier.¹⁶

Schwarz's measurements made use of the known equilibrium constants for the clustering reactions to deconvolute the absorption signal obtained at various pressures into those of individual ammoniated ammonium ions. These pioneering measurements, discussed later in the context of the results of the present study, suffered from limited spectral resolution (40 cm^{-1} full-width-half-maximum (FWHM)), relatively high vibrational and rotational temperatures (> 300K), and some ambiguity regarding the distribution of cluster sizes present in the sample. Nonetheless, it was possible for Schwarz to observe the vibrational bands ν_3 and $2\nu_4$ of the ammonium ion core for the n=4 cluster, and to show that the n=3 spectrum was consistent with C_{3v} symmetry. Schwarz was able to prove by isotope substitution that the structure of the n=4 ion cluster is tetrahedral. No transitions were observed that could unambiguously be assigned to the solvent molecules surrounding the ammonium ion.

Recently, we have studied the infrared vibrational predissociation spectroscopy of the tetra-ammoniated ammonium ion $\text{NH}_4^+(\text{NH}_3)_4$ using an arrangement of tandem mass spectrometers, a radio frequency ion trap and a tunable infrared laser.¹⁷ In addition to simply vibrational transitions, we have observed spectral features which are due to nearly free internal rotation of the ammonia subgroups in $\text{NH}_4^+(\text{NH}_3)_4$, the first observation of such a

phenomenon in an ionic cluster. This work also served to verify Schwarz's spectrum determined by deconvolution of the time dependent infrared absorbance based on equilibrium and rate constants, and his assignment of the ν_3 and $2\nu_4$ bands in the spectrum. The comparison with our spectra further indicates that the spectra we derive from vibrational predissociation are similar to those obtained by direct absorption for this system. In the present work we give a full account of our systematic investigation of a series of infrared vibrational predissociation (IRVPD) spectra of the ammoniated ammonium ions and present the absorption spectra for $\text{NH}_4^+(\text{NH}_3)_n$ ($n=1-10$) over the frequency range of 2600 to 3500 cm^{-1} .

It will be shown that correlation of spectral features with cluster size can provide information about solvation shell structure, the geometry of the clusters, and the onset of a condensed phase environment around the ion core. With sufficient laser resolution, rotational information about the cluster should also be obtainable with this new experimental technique.

EXPERIMENTAL DETAILS:

The experimental apparatus used in this work has been described previously.^{18,19,20,21} Briefly, the ammoniated ammonium cluster ions were produced from a high pressure corona discharge source and subsequent supersonic expansion. Schematic diagrams of the source and the experimental apparatus are shown in figs. 2 and 3. The corona discharge was maintained in 100-200 torr of gas (Matheson ultra high purity (UHP) neon typically seeded with 10% UHP H₂ and about 1% NH₃) flowing past a 1.2 KV potential from the discharge tip of the needle to the source body maintained at approximately 350 V above ground. The discharge current under these conditions ranged from 40-200 μ amps. The source could be cooled from outside the machine by contact with a liquefied gas reservoir and was usually maintained at approximately -30° C. After passing through the discharge region, the ionized gas undergoes collisionally induced vibrational relaxation in the 1.0 mm long by 3.0 mm diameter drift region before expanding through the 70 μ m expansion nozzle. It is estimated that an ion undergoes some 10⁵ collisions in this region before leaving the source, resulting in the ion relaxing to a vibrational temperature near that of the source body by the time it reaches the nozzle.

Most of the clustering of the neutral gas around the ionic species and rotational cooling takes place during the supersonic expansion between the nozzle and the skimmer. Typical pressures in the source chamber are 4×10^{-5} to 2×10^{-4} torr while running the experiment. To prevent internal excitation and dissociation of the

ionic clusters through collisions with the background gas in the expansion, the potential of the skimmer was maintained within 5 volts of that of the source body. A shielding grid surrounding the expansion region maintained at 350 V prevented stray fields from affecting the ion trajectories in this region.

After the skimmer, the ion beam enters a second differential pumping region containing collimating and focusing optics. The pressure in this second region is typically an order of magnitude lower than that of the source region. The beam is then directed into a third differentially pumped region maintained at 10^{-8} torr and through the entrance slits of a 60° sector magnet mass analyzer (Resolution = $M/\Delta M \approx 200$). To aid in transmission of the ion beam and to enhance mass resolution, a set of quadrupole lens pairs is placed before and after the magnet.^{22,23}

The mass selected beam passes into the final differentially pumped region maintained at 10^{-9} torr. Here, the beam is bent 90° in a DC quadrupole field, decelerated to less than 0.5 eV, and focused into a radio frequency (RF) octopole ion trap through an entrance aperture lens. Ions are typically allowed into the trap for 1 ms before the potential of the entrance lens is raised, and the ions confined inside the octopole.

The confined, mass selected clusters are then vibrationally excited by a pulsed, tunable infrared laser. (Quanta Ray, IR WEX 8 ns pulse, $0.3 - 1.2 \text{ cm}^{-1}$ resolution, 0.7 cm^{-1} absolute frequency accuracy, $0.2 - 1.0 \text{ mj/pulse}$ in the $2600-4000 \text{ cm}^{-1}$ region) The density of ionic clusters in the ion trap is not high enough to

allow the measurement of photon absorptions directly. In order to detect the absorption of an IR photon by an ionic cluster, IR multiphoton dissociation processes were used to exclusively dissociate the vibrationally excited ionic clusters. Depending on the density of states and the dissociation energy of the species under study, one of two excitation schemes described below was employed.

Because of the large binding energies of the $n=1$ and 2 ammoniated ammonium ions, absorption of sufficient energy from the tunable infrared (IR) laser to cause predissociation is not a facile process. In these cases, a line tunable CO_2 laser is used (MPB Technologies Inc. 8 W cw on R(24) of the $00^0_1-02^0_0$ transition) to drive the clusters excited by the tunable IR laser over the dissociation limit through the absorption of multiple CO_2 laser photons. This process hinges on the initial absorption of the tunable IR photon, as the density of states 1000 cm^{-1} above the $v=0$ level is so low that multi-photon dissociation of the ionic clusters by the cw CO_2 laser alone is very unlikely even with tens of milliseconds of irradiation time. In the studies of the $n=1$ cluster, no vibrational predissociation signal was observed if the pulsed laser was not present. Further discussion of this technique may be found elsewhere.²¹

For the larger clusters, $n=3-10$, the energy required to predissociate one solvent molecule is exceeded by absorbing two photons in the usual tuning range of $2.5-3.8 \mu\text{m}$. At an energy in the $2600-4000 \text{ cm}^{-1}$ region, all of the ionic clusters ($n=1-10$) are

literally in the "quasi-continuum" region²⁴ after the absorption of one photon and an additional IR photon from the tunable laser may be absorbed to induce vibrational predissociation. For $n=1$ and 2, however, fragments were not detectable with the tunable laser only, presumably because the fluence was not sufficient for the absorption of more than two photons. For these ions, use of the CO_2 laser with an irradiation time of at least 10 msec at >10 watts/cm^2 was required to achieve a measurable degree of dissociation of vibrationally excited clusters. In those instances where spectra of a given ion were obtained by both one and two color schemes, they were found to be the same within experimental error, indicating that spectral features in the multiphoton dissociation spectra normally reflect the cross section for absorption of the first photon rather well.²¹

If the clusters absorb sufficient energy through one of the schemes described above, the loss of one or more solvent molecules from the parent cluster may occur. The potential on the exit aperture is lowered 1 msec after the laser pulse, extracting cluster ions of all masses from the trap. These ions are filtered by a second mass analyzer, a quadrupole mass spectrometer tuned to pass only the daughter ions smaller than the parent cluster by one solvent molecule.

Daughter ions are counted using a Daly ion detector²⁵ for each laser shot. Background daughter ion counts resulting from the decay of metastable parent ions in the RF ion trap are monitored in a separate data cycle with the laser off at each wavelength, and

subtracted from the laser on signal. Typical background count rates usually amount to no more than 1% of the signal at the stronger absorption maxima. The spontaneous decay of metastable parent ions to daughter ions in the trap was as high as 5 % for the largest ions and as low as 10^{-2} % for $\text{NH}_4^+(\text{NH}_3)$.

Laser power is monitored at each data point and spectra are normalized for the tunable infrared power using a simple linear power dependence. For a typical experiment, signals were averaged for about 400 laser shots at each wavelength in the 2600 to 3200 cm^{-1} region and longer, about 1000 laser shots at each wavelength, in the 3200 to 4000 cm^{-1} region where signals were typically much weaker. This extra averaging is reflected in the better signal to noise ratios in the higher frequency region for some of the traces shown in fig. 9. Relative intensities between the two frequency regions should be correct.

RESULTS AND DISCUSSION:

A. Mass Spectra:

The distribution of ionic clusters produced by the corona discharge source could be shifted by altering the temperature of the source body, the backing pressure of the supersonic expansion, or the percentage of NH_3 in the H_2 carrier gas. Little dependence was observed between the peak of the cluster ion distribution and the magnitude of the current used in the discharge for a given value of the above parameters, indicating that the ions were at a reasonable equilibrium with the temperature of the source body before expansion through the nozzle.

The distribution of cluster sizes produced by the source could be easily monitored by sweeping the field of the 60 degree sector magnet and counting the ions that arrive at the Daly detector with the second mass filter set to transmit all ions. Two such mass spectra are shown in fig. 4. Spectrum 4a. was taken using a low concentration of ammonia in the H_2 carrier gas (<1%) , a backing pressure of 200 torr behind the nozzle and with the source body cooled to -30°C through contact with liquid freon 12. For these conditions the distribution shows a peak at the $n=4$ cluster. By cooling the source with liquid freon 22 (-40°C) instead of freon 12, and using a higher pressure behind the nozzle larger cluster ions could be favored as shown in 4c. Figure 4b. shows an intermediate condition. In this manner it was possible to produce in relatively high numbers the range of ionic cluster sizes desired for this study.

B. Notation for Spectral Assignments:

Of the various vibrational motions that take place within the ammoniated ammonium cluster ions, the only fundamental vibrational transitions accessible to the present laser system involve the high frequency N-H stretching motions. The numerous low frequency bending motions available to the cluster are in the case of this work observed only as overtone absorptions or in combination with a high frequency stretch. The higher frequency stretches we have assigned involve two types of N-H oscillators: those associated with the NH_4^+ core and those of the NH_3 solvent molecules.

For each of these, the frequency of a given transition for a particular subunit (either NH_4^+ or NH_3) will be shifted from that of the free molecule (or ion) by an amount determined by the local environment around the absorbing species. The normal modes of the NH_4^+ ion will be split into lower and higher frequency components due to the bound N-H's and higher frequency components associated primarily with bound and free N-H oscillators, respectively. Similarly, the NH_3 solvent molecules in the first solvation shell ($n \leq 4$) will be strongly influenced by NH_3 molecules in the second solvation shell and beyond ($n > 4$).

Because of the lengthy descriptions required to indicate the assignment of many of the vibrational bands, we introduce a shorthand notation: $Y_X^Z \text{ N-H}_P^Z$ to designate the subgroup involved in a particular transition and to describe the type of vibrational motion the subgroup undergoes. Under this notation, X takes on the values 0,1,2,... and indicates whether the subgroup is in the core,

first solvation shell, second solvation shell, etc., y is the number of equivalent N-H oscillators of a particular bond type in the local subunit, z is either bd (bound) or fr (free) to indicate whether the H of the N-H bond is involved in hydrogen bonding, and p is sstr, astr or bend depending upon whether the vibration can be considered as a symmetric or antisymmetric stretch, or a bending mode in the local subunit. If the symmetry of the stretch is not determined, but we still consider the transition a stretching type vibration we omit the "s" or the "a" in the notation. If a bond is directly affected by two attached subunits, where one of the subunits attaches to the other, z takes the form bd,bd. Our notational system can be used for spectra of other ion clusters as well, by adapting the N-H designation to indicate the appropriate bond type. Such a system treats the vibrational modes of each subunit separately from the rest of the complex. This "local subunit" approximation seems to work well for labeling spectra of weakly bound clusters, at least for the present spectral resolution. We will also use more conventional labels and full descriptions in many cases, reserving the most extensive use of the new notation for our table of assignments.

C. Infrared Vibrational Spectra:

In analyzing the infrared spectra of the ammoniated ammonium ion series, it is helpful to examine the general trends observed in the spectra before delving into a detailed investigation of individual cases. As implied by the notational scheme presented in the previous section, our approach has been to treat the various

subunits in the cluster as essentially isolated molecules (NH_3 or NH_4^+) perturbed by their particular environment. This approach is helpful from the standpoint of visualizing the types of vibrations involved in a given transition, and frees us from thinking of these large systems in terms of a normal-mode type of picture when the weak coupling between the subunits makes such an analysis difficult for all but the smallest clusters (e.g. $n=1$ and 2).

The spectra of the ammoniated ammonium ion series show a number of common features. Both absorptions due to the ammonium core stretches and those due to the ammonia solvent molecules can be assigned in every case. Features of the NH_4^+ core assigned to vibrations involved in hydrogen bonds with the solvent NH_3 's are strongly red-shifted from the gas phase values obtained from velocity modulation spectroscopy¹³⁻¹⁵ due to the strong interactions of the N-H bonds of the ion with the solvent molecules. Vibrational transitions involving the NH_3 molecules in the first solvation shell (1°) of the complex are significantly less perturbed from their gas phase values, however because the N-H bonds of the ammonias are not themselves involved in the hydrogen bond. This situation is changed for an N-H bond of the 1° ammonia which is involved in a hydrogen bond with a second solvation shell (2°) ammonia. A larger red-shift will take place for that N-H bond of the 1° ammonia, although not as large as that for the ion.

The spectral features due to the ion core in particular and to a lesser extent the solvent molecules show some systematic trends with increasing cluster size. The ion core frequencies associated

with extensive hydrogen bonding show a gradual blue shift. The amount of this shift is not constant with increasing solvation however, and in the extreme case of the largest clusters ($n=9-10$), the spectra change very little between the addition of one solvent molecule and the next, indicating that the core of the system is perhaps converging towards a liquid-like state.

The most striking feature of the spectra between 2600 and 3500 cm^{-1} for $n=1-6$ is a band originating at roughly 3400 cm^{-1} composed of a number of resolved subbands having a separation between adjacent components of about 12 cm^{-1} . This spacing is about twice the rotational constant for NH_3 about its C_3 symmetry axis and arises from the nearly free internal rotation of the 1° solvent molecules within the cluster. Observed previously in the $\text{NH}_4^+(\text{NH}_3)_4$ spectrum¹⁷, and assigned to a perpendicular band corresponding to the ν_3 mode of free NH_3 (See fig. 5), these transitions indicate that result that some of the solvent molecules in the first solvation shell are relatively unhindered even when the second solvation shell has begun to fill.

The assignments of the internal rotation subbands were given for $\text{NH}_4^+(\text{NH}_3)_4$ and are analogous for the corresponding bands of the other cluster ions. We use the notation for a strongly prolate symmetric top rotor in the table of assignments (See Table III) and in the text to describe the subbands. When the transitions $^R Q_3$ and $^P Q_3$ are observable, their intensities are consistent with the expected spin weight for transitions in NH_3 originating from $K=3$ levels. The only vibrational transitions for which the internal

rotor state of NH_3 will change are those involving modes of NH_3 with the selection rule $\Delta K=1$; here K is the quantum number for angular momentum about the NH_3 C_3 axis. (Our use of K and the notation R, P, Q_K , as we have stated previously,¹⁷ is not strictly correct. We use it for convenience, as the notation follows easily from the picture of NH_3 attached to a "wall", perpendicular to its C_3 axis. In the standard treatment presented here for the internal rotation observed in $\text{NH}_4^+(\text{NH}_3)$, both K and K_i the internal rotation quantum number must be used, and the symmetry and interaction of the rest of the molecule, must be included. There is no well developed theory for the treatment of the larger clusters.) No vibration of the ammonium core species carries this selection rule for angular momentum about one of the NH_3 C_3 axes; only a perpendicular vibration of the NH_3 subunit satisfies the condition. This includes the ν_3 type fundamental but not ν_1 (See fig. 5.) . It also includes the ν_4 type fundamental of NH_3 (the frequency is too low for us to observe) and perpendicular components of overtone and combination bands. The overtone $2\nu_4$ could therefore have shown the characteristic 12 cm^{-1} spacing, but did not. The most intense component of $2\nu_4$ is probably a parallel band. A detailed treatment of the internal rotation of the simpler $n=1$ cluster ion is given along more standard lines.

For $n \geq 4$, fundamental bands in the $3150\text{--}3500 \text{ cm}^{-1}$ region derive entirely from perturbed ammonia subunits. In the region $2600\text{--}3150 \text{ cm}^{-1}$, only vibrations associated with the NH_4^+ core appear. NH_4^+ is strongly hydrogen bonded via its hydrogen atoms, resulting in a

large redshift of the N-H stretching frequencies. The N-H vibrational frequencies in NH_3 shift relatively little when binding to the NH_4^+ core since the nitrogen atom of ammonia binds, rather than hydrogen. The hydrogen bonding between first shell (1° ; primary) and second shell (2° ; secondary) NH_3 is relatively weak, therefore the frequency shift of the bonded N-H stretch of 1° NH_3 is also relatively small. The separation of NH_3 and NH_4^+ vibrational bands for $n \geq 4$ in the $2600\text{-}3500 \text{ cm}^{-1}$ region is therefore easily understandable. This separation of core and solvent bands, taken together with the way in which several bond types form well-behaved series as a function of n , simplified the assignment process considerably.

The infrared absorption spectra for $\text{NH}_4^+(\text{NH}_3)_n$ ($n=1$ to 10) are discussed in detail below. Observed transition frequencies and assignments of the vibrational and rovibrational transitions observed in these spectra appear in Table III. Where available, observations from previous work are included in the table. Representative spectra for the $n=1$ to 8 ionic cluster series appear in figs. 6 and 9 and are discussed in detail for each cluster in the following text.

1. $\text{NH}_4^+(\text{NH}_3)$:

The smallest ionic cluster studied in this work is the ammonium ion solvated by a single ammonia. Bound with a ΔH° of formation of -27 kcal/mole , it is the most strongly bound of the ammoniated ammonium cluster ion series. Due to its small number of low frequency vibrational modes, the density of states²⁶ is

expected to be rather low at 3500 cm^{-1} . Like the analogous hydrated hydronium ion, it is important to know the equilibrium position of the proton between the two heavier nitrogen atoms. The two possible structures for this simplest cluster appear in fig. 7. In the C_{3v} structure, the proton is localized around one of the ammonias suggesting that the appropriate formulaic description of this system would be $NH_4^+(NH_3)$ whereas in the D_{3h} structure (D_{3d} is probably a more stable conformation by perhaps 10 cm^{-1}), it is equally shared suggesting that $(H_3N)H^+(NH_3)$ is the appropriate representation.

Ab initio calculations for the structure of the analogous $H_3O^+(H_2O)$ cluster ion suggested a double or single minimum for the proton position depending on the level of the calculation. The most sophisticated calculation to date is the as yet unpublished work of the Schaefer group in which the energies of the C_2 and C_s structures were found to have energies differing by no more than a few kcal/mole.²⁷ At the highest level of theory (full CISD-- configuration interaction including single and double excitations) the single minimum (symmetric $H_5O_2^+$ where the proton is at the midpoint of the oxygen atoms) was favored. At low levels of theory, the symmetric structure is usually favored also, but this order does not always hold.^{27,28,29,30,31} Spectroscopic investigations performed in this laboratory concluded that in this case the proton was centrally located,^{32,33} i.e., associated with a single minimum potential. Much evidence for the existence of such a structure in the solid and liquid phases has been presented

previously in the literature.³⁴ One of the most plausible proposals for the mechanism of proton transfer in aqueous acid solutions requires the existence of the symmetric structure at least as a transition state. Knowledge of the function which describes the potential energy for the proton as a function of its position and the O-O separation, is critical to understand and evaluate such a mechanism.

Theoretical calculations on $\text{NH}_4^+(\text{NH}_3)$ are significantly more primitive than those used for H_5O_2^+ , but predict N_2H_7^+ to have an asymmetric C_{3v} structure.^{35,36} The calculated energy difference, once again, is only a few kcal/mole. Given the margin for error in such a calculation and the fact that N_2H_7^+ and H_5O_2^+ are isoelectronic and obviously very similar molecules, such a conclusion cannot be accepted without verification. Both species have been theoretically studied extensively by Scheiner to determine the potential energy with respect to the proton position and the N-N or O-O separation. His results show that the potential and its form depend much more strongly on the N-N or O-O separation than the proton position, with respect to which the potential energy is extremely flat.

Assuming a symmetric structure (D_{3h} , see fig. 7b.) for this ion, the most intense absorption involving a high frequency N-H stretching motion would probably be the antisymmetric stretch of the NH_3 subunits. This motion, analogous to the ν_9 , ν_{13} modes in 2-butyne (dimethylacetylene) would give rise to a degenerate perpendicular transition of E_{1d} , E_{2d} symmetry. From the standpoint

of one of the ammonias, this motion is analogous to the doubly degenerate antisymmetric stretch, ν_3 , of free ammonia, which occurs at 3444 cm^{-1} in the gas phase³⁷ (See fig. 5). The asymmetric structure for the dimer, in contrast, (C_{3v} , see fig. 7a.) would have at least two types of antisymmetric stretching vibrations, one associated with the H-bonded NH_4^+ ion and one associated with the NH_3 molecule.

Schwarz detected a weak absorption as a shoulder at 3420 cm^{-1} that he assigned to this cluster. Any band arising from a stretching motion involving the hydrogen bonded proton evidently occurs below 2000 cm^{-1} , and was not observed. The transition we observed for this system appears in fig. 6a, and is centered at 3398.4 cm^{-1} , in reasonable agreement with the weak feature in Schwarz's spectrum at 3420 cm^{-1} . Schwarz assigned this to be ν_1 of the NH_3 subunit.

At the higher resolution available to this study, we found this band to be composed of a series of sub-bands spaced by $10.6 \pm 0.3 \text{ cm}^{-1}$. For a prolate symmetric top molecule with the rotational constants $A \gg B=C$, a strong Q-branch progression of this kind superimposed on vibrational transitions is commonly observed.³⁸ Spectra for molecules of this type, such as CH_3Br , have a characteristic separation between the Q-branch maxima of approximately $2(A-B)$.³⁹

For the structure observed in the N_2H_7^+ spectrum to be due to a simple rotation of the dimer however, the spacing of the subbands should be $\approx 5.6 \text{ cm}^{-1}$, based on the ab initio equilibrium

geometry.¹² The fact that the actual spacing is roughly twice as large and that similar structure was observed previously in the much larger $n=4$ cluster ($A=B=C \approx 0.1 \text{ cm}^{-1}$) suggests that these bands are due to an internal rotation of the NH_3 subgroups about their local C_3 axes, similar to that observed in $\text{NH}_4^+(\text{NH}_3)_4$.¹⁷

Internal Rotation in $\text{NH}_4^+(\text{NH}_3)_4$:

Internal rotation of molecules containing C_3 subgroups has been given extensive theoretical treatment.⁴⁰ Theories developed by Longuet-Higgins and Bunker⁴¹ and Papousek^{42,43} have been used to explain the structure in the antisymmetric stretching band, ν_9 , ν_{13} , in 2-butyne attributed to internal rotation of the methyl subgroups. In these theories, the rotational motion of the methyls through the three fold potential barrier is analyzed, taking into account the torsional barrier height, the degree of vibration-vibration coupling in the system, and the difference between upper and lower state rotational constants of the molecule. Using this approach, the ν_9 , ν_{13} band is reproduced to nearly the limit of experimental resolution. For 2-butyne, it was found that the barrier to internal rotation was small, less than 10 cm^{-1} .⁴¹⁻⁴⁴ Microwave spectra later demonstrated that the barrier to internal rotation was 5.6 cm^{-1} .⁴⁵

Exploiting the similarity between 2-butyne and the symmetric form of the N_2H_7^+ cluster ion, we have used the same formalism outlined by Papousek to simulate the antisymmetric stretching band, ν_3 . For an ethane-like molecule, Papousek derived the expression for the fundamental band of a perpendicular transition involving

E_{1d} and E_{2d} species. Frequencies for the fine structure transitions involved in the rotational Q branches of a transition from the ground vibrational state are given by the following:

$$\nu + \theta + \{A'(1 - 2\zeta_r^Z) - B'\} \pm 2[A'(1-\zeta_r^Z) - B']K \pm E(K_i).$$

Where:

$$\theta = [(A'-A'') + (B''-B')]K^2 + (A'-A'')K_i^2 + (B_i'-B'')J(J+1).$$

$$E(K_i) = 2A'(1-\zeta_r^Z)K_i + \Delta_v^2/[16A'K_i(\zeta_r^Z-1)].$$

In these expressions, the vibrational band origin is denoted by ν . A and B are the rotational constants of the molecule, and the single and double primes denote the excited and ground state constants, respectively. K and J are the usual rotational quantum numbers of the molecule. K_i is the torsional quantum number for internal rotation and B_i is the rotational constant of one of the rotating subgroups around its local C_3 axis. ζ_r^Z and Δ_v are the Coriolis coupling term and the vibration-vibration coupling term, respectively. Terms with the upper sign hold for $\Delta K = +1$, the lower for $\Delta K = -1$. For transitions from single-valued states, the quantum numbers K and K_i have the same parity, for transitions from the double-valued states, the opposite parity.

Selection rules for the perpendicular transition to the E_{1d} state should follow the selection rules: $\Delta J = 0, \pm 1$, $\Delta k = \pm 1$ ($K = |k|$) and $\Delta k_i = 0$ ($K_i = |k_i|$). More details may be found in Papousek (See refs. 41 and 42.).

In fig. 8a, a simulated spectrum calculated using the above expressions for $K = 0$ to ± 1 , $K_i = -9$ to $+9$, and $J = K$ to $K+9$ is

shown. The relative intensities of the lines in the spectrum are calculated from the Boltzmann factors, statistical weights of nuclear spin states and orientation factors of the ground vibrational state. A Lorentzian convolution of the line spectrum so generated is employed with a FWHM of 1.0 cm^{-1} to simulate the resolution of the machine function.

For this simulation the only parameters that were systematically varied were the vibrational band origin of the transition, ν , the rotational temperature of the molecule and the vibration-vibration coupling constant $\Delta\nu$. Values for the A' and B' rotational constants were selected assuming a symmetric structure. The excited state vibrational constant A'' was set at 3.16 cm^{-1} and B'' was set equal to B'. The Coriolis coupling constant and the torsional barrier height were both neglected. Values for the constants used appear in the figure caption.

One can see that in spite of the fact that the calculated spectrum does not include R and P branch structure, there is reasonable agreement with the experimental results in fig. 8b for the major features. Unfortunately, the shoulders present to the blue of the Q-branch maxima are not reproduced. For the R_{Q_K} series in a symmetric top, the R branch can be somewhat more intense than the P branch. Thus the weak feature at 3402 cm^{-1} may be attributable to an R branch of R_{Q_0} , as it peaks in the correct position for the expected rotational temperature of $\approx 20 \text{ K}$ and a rotational constant of 0.3 cm^{-1} .

There is certainly a possibility that these features might be

due to hot bands. A more likely explanation would be that this anomalous structure involves a rotation of the entire $\text{NH}_3\text{-H}^+\text{-NH}_3$ ion about its C_3 axis rather than just one NH_3 subunit about its local axis. As stated earlier, this structure would have half the spacing of the internal rotation structure, and could lead to peaks located roughly half way between the internal rotation Q branches. Such issues can be resolved by more detailed studies at higher spectral resolution which are presently underway.

The simulation seems successful in that the relatively large splitting in the $\Delta K=0$ and $\Delta K=-1$ subbands are reproduced, as is the smaller splitting in the $\Delta K=+1$ subband. This splitting arises in the simulation through the introduction of a small amount of vibration-vibration coupling into the energy expression through the Δv constant. The fact that the fit obtained for this spectrum did not require recourse to the formalism for a torsional barrier suggests, as in the case of 2-butyne, that the internal rotation is nearly free. That this should be the case is not entirely obvious from the standpoint of molecular geometries. In 2-butyne the distance between the hydrogens on different methyl substituents is about 4.9 Å. This distance is about 3.4 Å for the ab initio¹² structure $\text{NH}_4^+(\text{NH}_3)$ (about 0.2 Å less for the symmetric structure). The N-N distance in this ion is comparable to the N-C distance in the T-shaped van der Waals complex $\text{NH}_3\text{-CO}_2$, which also has a low barrier to internal rotation of less than 14 cal/mol.⁴⁶ From the relatively successful modeling of the spectrum in the same way as dimethylacetylene (See fig. 8.) and the strong dependence of the

appearance of the internal rotation bands on the torsional barrier height, we conclude that an upper limit to the torsional barrier height can be placed at about 10 cm^{-1} . In order to apply this theory to the larger clusters, it must be adapted for the particular geometry and the complete nuclear permutation inversion (CNPI) group.

The frequency of the central R_{Q_0} band for $n=1$ as compared to $n>1$ (these will be compared later) and the absence of two bands of comparable intensity (one each for " NH_4^+ " and " NH_3 " groups) suggest that, contrary to the ab initio results, the equilibrium structure of N_2H_7^+ is the symmetric one. With this configuration, the cluster would best be described by the formula $\text{H}_3\text{N}\cdot\text{H}^+\cdot\text{NH}_3$ rather than $\text{NH}_4^+\cdot\text{NH}_3$. It should be possible to determine the structure conclusively when a H_2 messenger study is performed as in the case of H_5O_2^+ and/or the spectrum is recorded at sufficiently high resolution to determine the rotational constant $B=C$. The rotational constant will allow an estimation of the N-N separation, which in turn should indicate whether the proton is equally shared by the nitrogens.

For the H_5O_2^+ system studied previously by a "messenger" technique, the small perturbation by a H_2 molecule on the H_5O_2^+ cluster is thought to lead to the formation of an asymmetric structure involving species similar to H_3O^+ and H_2O .^{47,48} Since the isolated H_5O_2^+ species is best thought of as $\text{H}_2\text{O}\cdot\text{H}^+\cdot\text{OH}_2$ rather than $\text{H}_3\text{O}^+\cdot\text{OH}_2$, the presence of the weakly bound "messenger" led to a dramatically different spectrum, providing qualitative confirma-

tion that the isolated H_5O_2^+ has a symmetric equilibrium structure. The definitive confirmation, of course, will probably come from a determination of the much lower vibrational frequencies involving the hydrogen bonded proton, as these are very sensitive to the structure.

2. $\text{NH}_4^+(\text{NH}_3)_2$:

The spectrum for the $\text{NH}_4^+(\text{NH}_3)_2$ cluster ion appears in fig. 6b. With a ΔH° of solvation of 17.5 kcal/mol for the $n=1 \rightarrow n=2$ clustering step⁷, this cluster is too strongly bound for two photons of 3000 cm^{-1} light to easily predissociate a solvent molecule unless a significant amount of internal excitation is already present. As in the case of the $n=1$ cluster, the two-color excitation scheme was used to study this system.

Ab initio calculations for the structure of the $n=2$ cluster by Hirao et al.¹² predict that the cluster should have the C_{2v} symmetry assumed by Schwarz. Alignment of the solvent ammonias along two of the four available binding sites in the first solvation shell yields an ammonium ion whose stretching vibrations can be roughly divided into two categories: hydrogen bonded and non hydrogen bonded. In the bonded category we have a symmetric and an antisymmetric mode, each involving the solvated core N-H bonds and appearing at relatively low frequency. In the nonbonded category we have a symmetric and an antisymmetric mode, each involving the unsolvated core N-H bonds and appearing at relatively high frequency. For the NH_3 solvent molecules, a symmetric stretch (ν_1) and a doubly degenerate antisymmetric stretch (ν_3) is expected;

these involve the three free N-H bonds of the NH_3 subunit (See fig. 5.). For this study, we will consider the vibrational bands of equivalent subunits in the complex to be degenerate for all ammoniated ammonium complexes.

Schwarz observed two broad peaks that he assigned to transitions involving modes of the NH_4^+ ion. A broad feature was observed in the $2400\text{-}2600\text{ cm}^{-1}$ region which was tentatively assigned to the low frequency N-H stretches, and a relatively narrow unidentified peak was observed at 2280 cm^{-1} . This latter peak we suspect may actually be the symmetric stretch of the two bound N-H oscillators. A higher frequency feature at 3360 cm^{-1} was assigned to the two free N-H stretches.

In this work, the low frequency peak lies below the lowest frequency accessible to the present laser system, but a series of transitions in the 3400 cm^{-1} region are observed. Shown in fig. 6b, Schwarz's peak around 3360 cm^{-1} is resolved into two main bands. The first, which seems to be split into two maxima at 3392 and 3395 cm^{-1} is assigned to the antisymmetric N-H stretches of the two free N-H oscillators of the ammonium core. Under the notational scheme discussed earlier, these bands would be designated ${}^2_0\text{N-H}_{\text{astr}}^{\text{fr}}$.

The symmetric stretch of these N-H bonds was not observed. This is not particularly surprising as it has been observed previously that the symmetric stretch of complexed ammonia has a particularly low infrared transition dipole moment.⁴⁹

A series of subbands is present slightly to the blue, with

similar structure as the feature in the $n=1$ spectrum and has been assigned to the ν_3 band of the ammonia solvent molecules. Under our new notation we would designate this band as ${}^2_1\text{N-H}_{\text{astr}}^{\text{fr}}$. With ${}^R_{Q_0}$ at 3413.7 cm^{-1} and an average spacing between adjacent components of $12.6 \pm 0.3 \text{ cm}^{-1}$, this structure is again due to internal rotation of the ammonia subgroups. For this cluster, where the perturbation of the NH_3 solvent molecules is less, the subband spacing agrees very well with the 12 cm^{-1} expected for free ammonia rotation about its C_3 axis. If the assignment of the ν_3 subbands is correct with respect to K , then this band falls nicely into the progression established by $n=1$ and $n=3-7$ (we will discuss this series in more detail later). However, this assignment appears to have some intensity anomalies; ${}^P_{Q_1}$, for example, appears much more intense than ${}^R_{Q_1}$. While this anomaly could possibly be due to an experimental artifact, one possible explanation is that the ν_3 state of the NH_3 subunits somehow interacts with the antisymmetric stretch of the free N-H oscillators of the core. Since the upper state of ${}^P_{Q_1}$ is about 25 cm^{-1} closer to this state than that of the upper level of ${}^R_{Q_1}$, ${}^P_{Q_1}$ is in a position to borrow more intensity. However, it is not clear why these levels should interact, and there is no corresponding frequency anomaly. A more attractive explanation is that the core antisymmetric stretching band is actually quite broad, $15-20 \text{ cm}^{-1}$, and therefore the intensity of ${}^P_{Q_1}$ appears large because it resides on the shoulder of this band. We therefore take ${}^R_{Q_0}$ at 3414 cm^{-1} as the most likely assignment.

3. $\text{NH}_4^+(\text{NH}_3)_3$:

The spectrum for the n=3 ammoniated ammonium ion appears in figs. 6c and 9a. The expected geometry should have roughly C_{3v} symmetry with the solvent molecules associating with three of the hydrogens on the central ammonium ion. Schwarz analyzed the vibrations for the NH_4^+ core under these conditions in terms of distorted T_d symmetry. Under this framework, six fundamentals are expected for the core, all infrared active. Of these, those that might be of a high enough frequency for the present laser system to excite are the stretching motions of the core; ν_1' , characterized primarily by the symmetric stretch of the hydrogen bonded core N-H's, ν_3' , the antisymmetric stretch involving the free N-H bond, and ν_3'' , the antisymmetric stretch involving the hydrogen bonded N-H's. Of these, ν_3' should appear at a higher frequency than either ν_1' or ν_3'' , which should have roughly the same frequency. One would also expect to observe transitions involving the solvent NH_3 's.

In fig. 9a, two strong absorptions are observed at 2660 and 2692 cm^{-1} , in agreement with Schwarz's low resolution observation of a single strong peak at 2682 cm^{-1} . Labeled with a 'B' in fig. 9a, these could be assigned to the fundamentals of the ν_1' and ν_3'' vibration discussed above. An alternative and somewhat more plausible assignment is that these two peaks, which are of equal intensity, arise from lifting the degeneracy of the ν_3'' doubly degenerate mode. The small peak at 2615 cm^{-1} is then taken to be ν_1' . Of course, a high quality ab initio calculation of the

intensities may be able to indicate which assignment is correct.

It is interesting to note that our spectrum of $n=3$ shows a very broad background absorption in the $2600-3100\text{ cm}^{-1}$ region which is so nearly featureless it is almost a continuum at our level of spectral resolution. When the spectrum was taken with a decreased backing pressure behind the nozzle resulting in a rotationally warmer expansion, the peaks broadened very much and the "continuum" became much more prominent relative to these peaks. A glance at Schwarz's $n=3$ spectrum indicates that the absorption is more intense in the 400 cm^{-1} region to the blue of the intense 2680 cm^{-1} peak than 400 cm^{-1} to the red, although in each case there is measurable absorption for the entire 400 cm^{-1} expanse. It will be seen later that the spectra of all the larger clusters show some absorption in the region above the ion core hydrogen bonded N-H stretches. We believe this to result from hot bands and combination bands involving these stretches and those of the hydrogen bonds themselves. The latter might be expected to have frequencies of $50-400\text{ cm}^{-1}$ for $n=2-10$, with the largest frequencies associated with the smallest values of n .

The free N-H stretching vibration ν_3' appears at 3374 cm^{-1} , again near the 3365 cm^{-1} measured by Schwarz. Also observed is the antisymmetric stretch of the solvent NH_3 's centered at 3416.8 cm^{-1} with the internal rotation structure observed previously (see fig. 6c for an expanded view of this region.). An inspection of the intensities of the Q-branches shows some enhancement in the $K=\pm 3$ stacks, consistent with the spin statistics expected for an ammonia

rotating about its C_3 axis.

4. $NH_4^+(NH_3)_4$:

Thermodynamic measurements and theoretical structural calculations indicate that the $n=4$ cluster ion represents the completion of the first solvation shell of the NH_4^+ ion. With four degenerate NH_3 solvent molecules, the cluster has the same T_d symmetry as the isolated ion core species^{14,15} (see fig. 10a). Therefore, only two fundamentals of the core should be infrared active: ν_3 , the triply degenerate antisymmetric stretch, and ν_4 , the doubly degenerate bending mode.

In the survey spectrum reported previously¹⁸ (See fig. 9b.), four main features are observed. The most prominent feature was assigned by Schwarz to the fundamental of the ν_3 vibration. The value from the present work of 2865 cm^{-1} agrees well with Schwarz's measurement of 2867 cm^{-1} for the position of this band. This band is connected to the analogous core vibration in the $n=3$ spectrum with a dashed line labeled 'B' in the figure.

Although the doubly degenerate ν_4 bending mode occurs at too low a frequency for either Schwarz or the present workers to measure (1400 cm^{-1} in matrices), Schwarz was able to observe the first overtone of the bending mode, $2\nu_4$, at 3087 cm^{-1} . This assignment was supported by an isotope substitution study in which a comparison of the Teller-Redlich product ratio⁵⁰ for the antisymmetric stretch and the bending overtones in NH_4^+ , ND_4^+ and CH_4 , CD_4 was made. In the present work, the $2\nu_4$ band is observed at 3095 cm^{-1} . Other bands are evident in the survey spectrum that

have been assigned to modes of the solvent NH_3 's.

As in the previous spectra, the antisymmetric stretching vibration of the first solvent shell ammonias is observed, centered at 3419.5 cm^{-1} with the structure due to internal rotation (See fig. 6d.) . With an average separation of 12.3 cm^{-1} between adjacent components, this band can be well fit to a model in which a single ammonia molecule is rotating freely about its C_3 axis attached to a "wall". In fact, the appearance of all the ν_3 bands for $n=3-6$ is very similar, so that all of them could be reasonably fit at the present resolution by the same model. Using a simple symmetric top expression for the position of the Q-branches, and the Hönl-London expressions for the transition intensities, this band has been fit to a rotational temperature of 35 K with respect to the K quantum number. The strong-weak-weak-strong intensity alternation expected for a molecule with C_{3v} symmetry is easily observed here. Intensities of subbands originating from $K=0$ and $K=3$ (R_{Q_0} , P_{Q_3} and R_{Q_3} in the figure) have about twice the intensity expected from the calculation just mentioned if nuclear spin statistics are not considered.

A second transition of the solvent molecules appears at approximately 3230 cm^{-1} and has been tentatively assigned to $2\nu_4$, the first overtone of the ν_4 bending mode. It is marked by a dashed line labeled 'D' in fig. 9b. There is a small possibility that the ν_1 symmetric stretching band overlaps with $2\nu_4$, but this is unlikely because it would require a much larger shift of the symmetric stretch in NH_3 upon complexation compared to that of the

antisymmetric stretch, 100 cm^{-1} vs. 30 cm^{-1} . Since the complexation of NH_3 generally results in a reduction of ν_1 intensity relative to ν_3 ,⁵¹ we believe that the ν_1 absorption is very weak and was consequently unobserved for $n=4$.

The disappearance of the 3374 cm^{-1} band in the $n=3$ spectrum which was assigned to the free N-H stretching motion of the core oscillator not bound by a solvent molecule, shows that the fourth solvent NH_3 indeed occupies the last first shell site on the NH_4^+ ion.

5. $\text{NH}_4^+(\text{NH}_3)_5$:

All of the thermodynamic and ab initio data are in agreement that the first solvent shell is filled at $n=4$. The ab initio calculation of Hirao et al¹² predicts that the fifth NH_3 hydrogen bonds to one NH oscillator of a 1°NH_3 . The spectrum of $n=5$ shows conclusively that this is correct. There is strong support for this picture of the binding that leads to the weakening of one core NH oscillator and strengthening of the other three.

The NH_3 attached to the first solvation shell alters both spectral features associated with the NH_4^+ ion core of the cluster and the first solvation shell (1°) ammonia that this second solvation shell (2°) NH_3 is bound to. For the $n=4$ cluster, the ν_1 symmetric stretching vibration is not infrared active due to the T_d symmetry of the environment around the core and the core itself. By adding another NH_3 outside the first shell, this motion should become weakly IR active. Similarly, the triply degenerate antisymmetric stretch of the core, ν_3 , will split into a doubly

degenerate antisymmetric stretching component of higher frequency, ν_3' , similar to that for the $n=4$ cluster, and a lower frequency component, ν_3'' , dominated by the N-H stretching motion of the core bound to both a 1° and a 2° NH_3 .

In the spectrum shown in fig. 9c for the $n=5$ cluster, the small, sharp feature observed at 2890 cm^{-1} and labeled 'C' is assigned to the symmetric stretching motion of the core, ν_1' . The weak intensity of this band is consistent with the only slight breaking of the symmetry of the core by the 2° ammonia.

Another new, broad feature centered at 2650 cm^{-1} , labeled 'A' in the figure, is correlated with the addition of an NH_3 into the second solvation shell. The fact that this feature greatly increases in relative intensity as the number of solvent molecules increases beyond $n=5$ (see the following section), lends support to the notion that it involves a vibration coupled to the second solvation shell ammonias. We assign it to the low frequency component of the antisymmetric stretch of the core, ν_3'' . The large width of the feature ($50\text{-}60 \text{ cm}^{-1}$ FWHM) even at the low rotational temperatures of this study suggests that extensive hydrogen bonding is involved. The intense 2910 cm^{-1} band, 'B', also associated with an oscillator involved in hydrogen bonding, is relatively narrow (25 cm^{-1} FWHM). This peak can be clearly assigned to ν_3' . The smaller width of this band, even when compared to ν_3 in $\text{NH}_4^+(\text{NH}_3)_4$, correlates with the strength of the hydrogen bonding interaction.

A series of weak absorptions appear in the $3000\text{-}3200 \text{ cm}^{-1}$ region. The group of two peaks centered at 3010 cm^{-1} and an

additional set of two peaks centered at 3110 cm^{-1} probably correlate to the features in the $n=4$ spectrum at 3010 and 3095 cm^{-1} , respectively. There, the identity of the first feature was uncertain, and there was strong evidence from Schwarz that the second was due to the first overtone, $2\nu_4$ of the triply degenerate bending mode of the core. Based on the latter identification, we tentatively assign the 3110 cm^{-1} group to a similar bending motion. Because of the loss of degeneracy produced by the second shell ammonia, the bending mode can be expected to split into a high frequency and a low frequency component, the lower of which would probably be most closely associated with the three equivalent core oscillators. A splitting of 30 cm^{-1} , as observed, does not seem unreasonable. The 3010 cm^{-1} set of peaks is presumably an overtone or combination band. One possibility is a combination of the ν_1' and intense ν_3' modes (2890 and 2910 cm^{-1} peaks) with the intense low frequency hydrogen bond stretching modes. This would place the stretching frequency of the three equivalent hydrogen bonds at about 110 cm^{-1} , which also does not seem unreasonable. Another possibility is that these peaks are due to a bending overtone of the core oscillator with attached 1° and 2° NH_3 ligands. In this case, the 3110 cm^{-1} group would be assigned to the bending overtone of the other three oscillators.

The addition of an NH_3 into the second shell should also have an effect on the 1° ammonia to which it attaches. If the bonding occurs through the sort of hydrogen bond illustrated in figure 10b, one would expect the 12 cm^{-1} characteristic spacing of free

internal rotation of 1°NH_3 to disappear when the 1°NH_3 is bound to a 2°NH_3 . The antisymmetric stretching motion of the 1° solvent molecule would also be split into a low frequency hydrogen bound component and two higher frequency free N-H stretching motions: a symmetric stretching component and an antisymmetric one.

Centered at 3419.8 cm^{-1} and shown in expanded view in fig. 6e is the now familiar structure due to internal rotation of the 1°NH_3 's superimposed on the antisymmetric stretching vibration of the subgroups. Band 'E' in fig. 9c, at 3364 cm^{-1} , however, is a new feature not observed for $n=4$, and arises from the presence of the 2°NH_3 . The frequency is appropriate for NH oscillators which are not hydrogen bonded. This band is significantly broader than the individual components of the $\text{NH}_3 \nu_3$ band, and shows no rotational structure at this level of resolution. It is assigned to the free N-H antisymmetric stretching motion of the 1°NH_3 bound to the 2°NH_3 , denoted ${}^2_1\text{N-H}_{\text{astr}}^{\text{fr}}$ in the new notation.

The band labeled 'D' in fig. 9c centered at 3230 cm^{-1} , has gained considerably in intensity from $n=4$ to $n=5$. We assign this feature to two overlapping bands, one due to the bound N-H oscillator of the 1°NH_3 , ${}^1_1\text{N-H}_{\text{str}}^{\text{bd}}$. The other band is due to $2\nu_4$ of the three equivalent unbound 1°NH_3 subunits, although the remaining 1°NH_3 and the 2°NH_3 may also contribute intensity by N-H bending overtones. By $n=6$, we certainly expect the majority of intensity in the solvent region of the spectrum to come from the N-H stretch of 1° hydrogen bonded oscillators, although we cannot rule out significant contribution from bending overtones. Once

again, ab initio calculation might help to clarify this. It seems, however, that the structure of n=5 is of the sort given in figure 10b. It is also clear due to the lack of the 3370 cm^{-1} feature found in the n=5 to 8 spectra, that in the n=4 spectrum there is essentially no n=4 isomer with a $1^\circ\text{-}2^\circ\text{ NH}_3$ hydrogen bond.

The contribution of the outer shell NH_3 N-H oscillators to the n=5 spectrum is minor and could not be identified. When the n=8 spectrum is discussed later, however, it will be suggested that the barrier to internal rotation is higher for outer NH_3 subunits in n=5-8 complexes than for nonbonded 1° NH_3 in n=1-7 complexes.

6. $\text{NH}_4^+(\text{NH}_3)_6$:

As the number of solvent molecules around the NH_4^+ increases, the production of isoenergetic conformers becomes more likely. A consequence of this is that speculations about the detailed structure of the larger ammoniated ammonium ions becomes less certain. However, it seems reasonable to suppose that the structure of the first solvation shell is reasonably well-preserved and that the addition of subsequent ammonias tends to occur predominantly through the sort of hydrogen bonding scheme discussed in the previous section. The spectra are found to be consistent with this assumption.

Working from the premise that additional solvent molecules bind to successive first shell ammonias, we presume that by the n=6 cluster two of the four available second shell sites are occupied. Using the n=5 cluster as a model for the spectrum, we would expect the components of the core vibrational band assigned to a

stretching motion where N-H bonds of the core are bound to both a 1° and a 2° NH₃ (${}^2_0\text{N-H}_{\text{str}}^{\text{bd, bd}}$) to increase in relative intensity. Conversely, the feature associated with the antisymmetric stretch of the core bound only to 1° ammonias should decrease in relative intensity (${}^2_0\text{N-H}_{\text{astr}}^{\text{bd}}$).

A glance at fig. 9d shows that this is the case, as peak 'A' increases dramatically in intensity relative to peak 'B'. Recall that 'A' was first observed in the n=5 spectrum and is therefore associated with the onset of the second solvation shell. In addition to a sharp increase in intensity, it has also shifted to higher frequency, 2720 cm⁻¹. Again, this band is assigned to a stretching motion of the core where the N-H bonds involved are themselves bound to both a 1° and a 2° NH₃ (${}^2_0\text{N-H}_{\text{astr}}^{\text{bd}}$). We call it an antisymmetric stretch because symmetric stretches, in general, seem to carry less intensity. At 2920 cm⁻¹, the symmetric stretching motion of the core oscillators bound to only 1° ligands is observed (${}^2_0\text{N-H}_{\text{sstr}}^{\text{bd}}$), and is labeled 'C' in fig. 9d. The antisymmetric stretching motion of the same core oscillators, ${}^2_0\text{N-H}_{\text{astr}}^{\text{bd}}$, is observed at 2950 cm⁻¹ and labeled 'B'. A broad band whose maximum occurs at 3020 cm⁻¹ is observed and is tentatively assigned to the first overtone of the overlapping core bending modes ${}^2_0\text{N-H}_{\text{bend}}^{\text{bd, bd}}$ and ${}^2_0\text{N-H}_{\text{bend}}^{\text{bd}}$, with a possible contribution from a combination band involving ${}^2_0\text{N-H}_{\text{str}}^{\text{bd}}$ and the hydrogen bond stretch.

The effect of further occupation of the second solvation shell should also have an effect on the spectroscopy of the first

solvation shell ammonias. The structure due to internal rotation of the 1° solvent molecules is still observed, but at much lower relative intensity. With R_{Q_0} centered at 3422 cm^{-1} , this structure lies slightly to the blue of the analogous n=4 and 5 bands (See fig. 6f.). The structure assigned to the free N-H antisymmetric stretching motion of the 1° ammonias bound by the second solvation shell ammonias ${}^2_1\text{N-H}_{\text{astr}}^{\text{fr}}$, 'E' in fig. 9d, has greatly increased in relative intensity, and appears at 3368 cm^{-1} . Similarly, the ${}^1_1\text{N-H}_{\text{sstr}}^{\text{bd}}$ mode has increased in intensity and appears at 3225 cm^{-1} . This feature is labeled 'D'.

The weak feature at about 3320 cm^{-1} is probably the symmetric stretch ν_1 of the two 2° ammonias, overlapped with the symmetric stretch of free N-H oscillators of those 1° subunits with an attached 2° NH_3 . There is a slight indication that a very weak band is present here in the n=5 spectrum as well. While the ν_1 and ν_3 bands in isolated NH_3 have comparable intensity, it has been clear that in the complexes n=1-5 the ν_3 band of NH_3 subunits carries much more intensity than ν_1 . The appearance of ν_1 at n=6 with comparable intensity to ν_3 could then be taken as an indication of how weakly the second shell NH_3 subunits are bound. The 3320 cm^{-1} band, upon close inspection, seems to consist of two peaks at 3310 and 3325 cm^{-1} . A careful comparison of the n=7 spectrum in the same region reveals similar structure. By analogy with the symmetric stretch observed in the spectrum of liquid ammonia⁵² at 3300 cm^{-1} and similar structure observed in clusters of neutral ammonia clusters⁵³, we tentatively assign the 3310 cm^{-1}

peak to the symmetric stretch of primary subunits, $2_1^\circ\text{N-H}_{\text{sstr}}^{\text{bd}}$. By analogy to ν_1 in isolated NH_3 , we tentatively assign the 3325 cm^{-1} peak to ν_1 of the two second shell ammonias. The two remaining first shell unbound ammonias are presumed to constitute a minor contribution.

7. $\text{NH}_4^+(\text{NH}_3)_7$:

It is obvious how most of the $n=7$ features in fig. 9e correlate with $n=6$ in fig. 9d. Most of the difference in appearance of the two spectra has to do with the modes of the NH_4^+ core at frequencies below 3100 cm^{-1} . It is very obvious that the intense 2770 cm^{-1} peak of $n=7$, 'A' in the figure, correlates with the 2720 cm^{-1} peak of $n=6$ (it will be shown later that the two peaks fall into a smooth frequency progression established by the other clusters), and we readily assign it as $3_0^\circ\text{N-H}_{\text{astr}}^{\text{bd},\text{bd}}$. The FWHM of the band is about 80 cm^{-1} , slightly less than for the analogous band in $n=6$. This reduction is consistent with the lower hydrogen bond strength in $n=7$. The intense 2950 cm^{-1} peak in $n=6$ and its companion at 2920 cm^{-1} ('B' and 'C' in fig. 9d.) have nearly disappeared in the $n=7$ spectrum. It is expected from our $n=6$ assignments that these two peaks should collapse into one peak of reduced intensity for $n=7$, if the cluster consists of an NH_4^+ core, four first shell NH_3 subunits and three second shell NH_3 subunits each hydrogen bonded to its own primary subunit. In fact, it appears that the peaks do collapse, and the reduction in intensity is surprisingly dramatic. In the spectra of the higher ammoniates, such a peak is not observed, suggesting that all of the

N-H bonds of the ammonium core are experiencing hydrogen bonding with both 1° and 2° solvent molecules.

The only new feature appears at 2870 cm^{-1} and is quite weak. This band is more prominent in the n=8 spectrum. Our very tentative assignment is to a combination band involving the core stretching mode ${}^3_0 \text{N-H}_{\text{astr}}^{\text{bd, bd}}$, and the hydrogen bond to these three equivalent oscillators. If correct, this assignment places the frequency of this strongest of the hydrogen bonds in n=7 at about $70\text{-}90 \text{ cm}^{-1}$.

The band centered at 3050 cm^{-1} seems to be a bending overtone of the three equivalent N-H oscillators. The remaining features at 3020 and 2990 cm^{-1} might be produced by bending overtones of other N-H oscillators.

From the above discussion, it seems that the lowest energy structure consists of an NH_4^+ core with four 1° NH_3 ligands and three 2° NH_3 ligands, each attached to a different 1° subunit. There is no definitive indication for the symmetric structure $(\text{NH}_3)_3(\text{N}_2\text{H}_7^+)(\text{NH}_3)_3$, analogous to the species $(\text{H}_2\text{O})_2(\text{H}_5\text{O}_2^+)(\text{H}_2\text{O})_2$ which is proposed to be an intermediate in proton transfer²⁹, nor any other isomer. There is also no strong indication for a "cross-linking" of second shell ammonia to another ammonia subunit in the first or second shell, with the formation of large ring structures. It is clear from the ν_3' band of the propellering first shell NH_3 that this subunit is not involved in cross-linking. If there is cross-linking of two second shell ammonias, however, it may be difficult to discern from the spectrum due to the weak absorptions

of these subunits and the possibility that the absorptions may overlap with those of primary ammonia.

8. $\text{NH}_4^+(\text{NH}_3)_{8-10}$:

One would expect that as the number of NH_3 molecules around the NH_4^+ increases, the spectrum of the ammoniated ammonium ion cluster should eventually converge. In the limiting case, this spectrum would be that of an ammonium ion solvated in a liquid ammonia environment. Spectral features associated with an ammonium ion bound to both 1° and 2° amonias should further increase in relative intensity. Conversely, NH_4^+ stretches involved in bonding to 1° NH_3 's only, should disappear at $n=8$ provided that the second shell, like the first shell, is filled by four ligands each bound to a separate primary ammonia. For the 1° NH_3 molecules, free rotation as observed in the $n=1$ to 6 spectra should be quenched for $n>7$. A similar band structure could take its place, but associated with 2° NH_3 . Absorptions due to second and third shell ammonia might be very apparent by $n=10$. Stretching vibrations of the solvent subunits should begin to approach those observed in the condensed phases. Unfortunately, spectra for the $n=9$ and 10 clusters were limited by low signal to noise ratio to the 2600 to 3200 cm^{-1} region because of the weak absorbance in the higher frequency region and the low number density of larger mass clusters obtainable.

The IRVPD spectra for the $n=8$ ammoniated ammonium ion cluster appears in figs. 6g and 9f. For the higher ammoniates, the spectra are essentially the same as that of the $n=8$ species. Band maxima

for the features observed in the n=8 to 10 spectra are listed in Table III.

Once again, the assignments stem from those of the smaller clusters. The very intense peak at 2830 cm^{-1} , 'A', is an antisymmetric stretch of the core N-H oscillators, which is analogous to the triply degenerate ν_3 fundamental of NH_4^+ or $\text{NH}_4^+(\text{NH}_3)_4$. The weaker absorption centered at 2900 cm^{-1} , and first observed for n=7 at 2870 cm^{-1} , is probably a combination band of the ν_3 mode with the stretching mode of the hydrogen bonds between core and 1° ammonias. The peak at 3050 cm^{-1} is assigned to the bending overtone of the core, $2\nu_4$.

The major difference in the spectra of n=9 and 10 in the $2600\text{--}3200\text{ cm}^{-1}$ region from that of n=8, lies in the slight blue shift of the intense band at 2820 cm^{-1} for n=8. It appears at 2829 and 2841 cm^{-1} in the n=9 and 10 spectra, respectively. The frequencies of other bands have converged more quickly.

Intensities and positions of peaks in the $3200\text{--}3500\text{ cm}^{-1}$ region differ only slightly from the n=6 spectrum with the notable exception of the internal rotation structure, which is absent. The 3220 cm^{-1} peak ('D' in fig. 9f) is assigned primarily to $4^1\text{N-H}_{\text{astr}}^{\text{bd}}$, with perhaps contributions from $2\nu_4$ of 2°NH_3 . We believe the 3320 cm^{-1} peak to be ν_1 of 2°NH_3 , with the weak shoulder at 3300 cm^{-1} attributed to the symmetric stretch of the two equivalent N-H bonds of the 1°NH_3 subunits. The peak at 3380 cm^{-1} ('E' in fig. 9f) is easily assigned to the antisymmetric stretch of the two equivalent N-H bonds of the 1° subunits bound by 2°NH_3 's.

The appearance of the band which peaks at 3415 cm^{-1} is very different from that of the smaller clusters in the same region. The structure observed for $n=7$ was similarly weak and began to appear a bit broadened, but sharp structure from internal rotation of the 1° NH_3 's was still apparent. The corresponding band for $n=8$ shown in fig. 6g is unmistakably broadened, shifted slightly to the red and no structure due to internal rotation is evident. (Due to the weak signal for this cluster, a larger wavelength increment between data points and longer averaging time at each point was used for this trace. Spectral resolution is slightly larger than 1 cm^{-1} , but is still well inside the expected 12 cm^{-1} structure for internal rotation.)

It appears that this feature is actually the ν_3 band of 2° NH_3 . Evidently the 2° subunits are not able to propeller in the same manner as the 1° NH_3 's. The latter suggestion is supported, as the loss of structure and a red shift of about 6 cm^{-1} would be expected for NH_3 subunits with a relatively high barrier to internal rotation. It is quite possible that the 2° NH_3 's do not attach via a linear hydrogen bond thereby resulting in an orientation not along the 2° NH_3 's local C_3 axis. It is known from microwave spectroscopy that the neutral ammonia dimer is not held together by a hydrogen bond.⁵⁴ If something similar is happening in these large clusters, a larger barrier to internal rotation could result. Cross-linking between 2° subunits would also explain the loss of internal rotation structure.

Another explanation for a higher internal rotation barrier of

2° NH_3 as compared to unbound 1° NH_3 is related to the low symmetry of 1° NH_3 compared to the NH_4^+ core. When a 2° NH_3 attaches to 1° NH_3 with its C_3 axis coincident with an NH bond vector of the 1° subunit, that 1° subunit has only two equivalent N-H bonds. The potential function for internal rotation of 2° subunits therefore seems likely to be more complicated, with perhaps a somewhat higher barrier. In any case, there seems to be no doubt that the dominant structure involves 4 1° NH_3 ligands and 4 2° ligands, each attached to a different 1° subunit. Our preferred structure for the $\text{NH}_4^+(\text{NH}_3)_8$ complex is that shown in fig. 10c.

SUMMARY AND CONCLUSIONS:

The infrared vibrational predissociation spectra of the ammoniated ammonium ions contain two main classes of spectral features: those that can be assigned to motions of the NH_4^+ ion core of the cluster, and those that can be attributed to the NH_3 solvent molecules. The core vibrations observed can be easily understood in terms of the ν_3 (antisymmetric stretch), ν_1 (symmetric stretch) and $2\nu_4$ (degenerate bending) modes of the NH_4^+ ion in several cases, with the application of distorted tetrahedron theory. The most prominent solvent vibrations that are observed are assigned to transitions arising from the first solvent shell (1°) ammonias; transitions of second shell (2°) subunits account for relatively weak features appearing only in the spectra of the largest clusters. For the 1° NH_3 molecules not perturbed by second solvation shell (2°) NH_3 's, the strongest transitions assigned are analogous to ν_3 (the doubly degenerate antisymmetric stretch) and $2\nu_4$ (the bending mode) of NH_3 . For the ν_3 -type mode, rotational structure is observed on the vibrational transition that has been assigned to an internal rotation of the ammonias about their local C_3 axes. The internal rotation structure is observed as a consequence of the selection rule $\Delta K = \pm 1$ for this perpendicular band (perpendicular with respect to the C_3 axis of the NH_3 subunit whose ν_3 vibration is excited), where K is the quantum number for angular momentum about the NH_3 C_3 axis. Such a structure is also expected for the ν_4 fundamental, but not for the ν_1 or ν_2 modes.

Trends in the measured vibrational frequencies are observed

for both core and solvent vibrations in the $\text{NH}_4^+(\text{NH}_3)_n$ species which converge at large n . The ν_3 antisymmetric stretching vibration for the 1° solvent molecules was first observed in the $n=1$ cluster. With R_{Q_0} centered at 3398.4 cm^{-1} , this feature shifts further to the blue and decreases in relative intensity with increasing cluster size. The frequencies of the central R_{Q_0} ($K = 0$) bands measured for this transition are plotted as a function of cluster size in fig. 11a. The band origins in each case lie about 6 cm^{-1} to the red of the listed frequency. The band origin of free NH_3 in the gas phase is 3444 cm^{-1} . (See Table I. Reference e.) It can be seen that, as in the case of other cluster ions observed previously, such as the hydrogen cluster ions, H_n^+ and the hydrated hydronium ions, the converged value of this solvent transition lies significantly below the value for the free molecule due to the red-shift imposed by the solvation interaction even at large distances from the ion core.

A similar plot for the frequencies of the antisymmetric stretching vibration of the core bound to only 1° NH_3 's is shown in fig. 11b. The first point in the plot for the $n=2$ cluster is from Schwarz's measurement which he tentatively assigned to the component of the antisymmetric stretch of the NH_4^+ ion bound by two NH_3 's. We observe the analogous feature in the $n=3-7$ spectra shift to the blue and decrease in relative intensity, converging by the $n=7$ spectrum to 2989 cm^{-1} . The frequencies for similar core stretching vibrations with an attached 2° NH_3 as well, are plotted in fig. 11c.

The spectra have clearly indicated, in agreement with previous thermochemical measurements and theoretical calculations, that a well-defined shell structure exists. The first solvent shell is completed by four ligands. The fifth ligand hydrogen bonds to a 1° NH₃, with only one N-H bond of the 1° subunit directly affected. Successive ammonia ligands hydrogen bond to other 1° subunits in the same way until the n=8 complex shown in fig. 10c is obtained. In this complex each 1° subunit is bound by one 2° subunit.

In the complexes n=1-7, any 1° NH₃ which is not bonded to a 2° subunit has a ν_3 band which exhibits the structure characteristic of nearly free internal rotation of that 1° subunit. A 1° NH₃ which is bonded to a 2° subunit might well undergo internal rotation, but the characteristic spacing of the Q-branches in the associated ν_3 band will be less than the 1 cm⁻¹ laser linewidth employed for these studies. For the 2° NH₃, the barrier to internal rotation about the local C_{3v} axes evidently is higher, or the transition fails to carry sufficient oscillator strength to be observed, as the spectrum of the n=8 cluster indicates no such structure.

For the n=9 and 10 complexes, it is not yet clear what binding sites(s) the outermost ligands occupy. If they attach to 2° NH₃ subunits, one would expect a new band to appear, red-shifted by perhaps a hundred wavenumbers from the core ν_3 stretch at ≈ 2830 cm⁻¹. This is not observed. It may be that the 9th and 10th ligands attach loosely to 1° NH₃ subunits. Therefore, although we believe that some sort of shell structure is completed at n=8 (NH₄⁺(NH₃)₈),

this structure is not so well defined as that filled at $n=4$. We could, for example, say that the 9th and 10th ligands enter the 2' shell rather than 3; the second shell might be $1/3$ or $1/2$ full when it contains 4 ligands. In any case, it is useful to note that the convergence plot of fig. 11c seems to show a slight kink at $n=8$, with such small frequency shifts for $n=9,10$ that the binding of these ligands is apparently quite weak.

The spectra which were obtained for $n=9-10$ are quite similar to that of $n=8$, indicating that the NH_4^+ core, at least, is affected only slightly in its infrared absorption properties by the addition of these ligands. Of course, there may be other properties of the core or of the rest of the complex, which are more significantly affected. The infrared probe is sensitive to bond length and bond strength, and we can say that these characteristics of the NH_4^+ core are no longer changing. It is probable that these properties are likely to show significant discontinuities for certain larger values of n , if special structures form.

A comparison of the spectra of ammonium salts with weakly interacting counter ions such as NO_3^- or ClO_4^- in ammonia solution with that of the $n=8$ ionic cluster shows unmistakable similarity, particularly at low temperatures. For the more strongly interacting counter ion Cl^- , the spectrum is still very similar, especially for a mole ratio $\text{NH}_3:\text{ClNH}_4 \geq 6$ (See fig. 2 of ref. 3.). In general, the broad, intense absorption in the 2800 cm^{-1} region of ammonium salts should be associated with a ν_3 type vibration of solvated NH_4^+ . In the $3200-3500 \text{ cm}^{-1}$ region, the spectrum is quite

similar to that of liquid ammonia⁵² or neutral ammonia clusters $(\text{NH}_3)_n$ ($n=3-5$)⁵³. So far as the infrared spectra are concerned, the $n=8$ complex is already quite close to an NH_4^+ in a liquid-like environment. In other words, the very strong "chemical-like" bonding of the NH_4^+ to the solvent molecules gets diluted over the large number of subunits by $n=8$ so that the interaction of the ionic core with additional NH_3 's is comparable to that between neutral NH_3 's.

While the spectra of crystalline ammonium salts have been well understood for many years, that of the same salts in NH_3 solution has been more difficult to interpret. The liquid phase vibrational bands tend to be very broad, even when compared to those of the solid phase, and the relative intensities of the bands can vary dramatically with the chemical conditions. The spectra of cold ammoniated ammonium clusters in the gas phase can therefore contribute a great deal to our understanding of the interactions present in such solutions.

Acknowledgement

This work was supported by the Director, Office of Energy Research, Office of Basic Energy Sciences, Chemical Sciences Division of the under Contract No. DE-AC03-76SF00098.

REFERENCES:

1. E.L. Wagner and D.F. Horning, *J. Chem. Phys.* **18**, 296 (1949).
2. J. P. Mathieu and H. Poulet, *Spectrochim. Acta A* **16**, 696 (1960).
3. J. Corset, P. V. Huong and J. Lascombe, *Spectrochim. Acta A* **24**, 2045 (1968).
4. A. M. Hogg and P. Kebarle, *J. Chem. Phys.* **43**, 449 (1965).
5. A. M. Hogg, R. M. Haynes, and P. Kebarle, *J. Am. Chem. Soc.* **88**, 28 (1966).
6. S.K. Searles and P. Kebarle, *J. Phys. Chem.* **72**, 742 (1968).
7. J. D. Payzant, A. J. Cunningham and P. Kebarle, *Can. J. Chem.* **51**, 3242 (1973).
8. I. N. Tang and A. W. Castleman Jr., *J. Chem. Phys.* **62**, 4576 (1975).
9. M. R. Arshadi and J. H. Futrell, *J. Phys. Chem.* **78**, 1482 (1974).
10. S. T. Ceyer, P. W. Tiedemann, B. H. Mahan, and Y. T. Lee, *J. Chem. Phys.* **70**(1), 14 (1979).
11. A. Pulman and A.M. Armbuster, *Chem. Phys. Lett.* **36**, 558 (1975).
12. K. Hirao, T. Fugikawa, H. Konishi, and S. Yamabe, *Chem. Phys. Lett.* **104**, 184 (1984).
13. C. S. Gudeman and R. J. Saykally, *Ann. Rev. Phys. Chem.* **35**, 387 (1984).
14. M. W. Crofton and T. Oka, *J. Chem. Phys.* **79**, 3157 (1983); **86**, 5983 (1987).
15. Eckhard Schafer and Richard J. Saykally, *J. Chem. Phys.* **80**(9), 3969 (1984).
16. H. A. Schwarz, *J. Chem. Phys.* **72**, 284 (1980).
17. J. M. Price, M. W. Crofton and Y. T. Lee, *J. Chem. Phys.* **91**, 2749 (1989).
18. S.W. Bustamente, Ph.D. Thesis, Univeristy of California at Berkeley, (1983).

19. S.W. Bustamente, M. Okumura, D. Gerlich, H. S. Kwok, L. R. Carlson, and Y. T. Lee, *J. Chem. Phys.* **86**, 508 (1987).
20. M. Okumura, Ph.D. Thesis, University of California at Berkeley, (1986).
21. L. I-C. Yeh, Ph.D. Thesis, University of California at Berkeley, (1988).
22. H.A. Enge, *Rev. Sci. Instrum.* **30**, 248 (1959); C.F. Giese **30**, 260 (1959); C-S. Lu and H.E. Carr **33**, 823 (1962).
23. S. Taya, I. Kanomatata, H. Hirose, T. Noda, and H. Matsuda, *Int. J. Mass Spectr. and Ion Phys.* **26**, 237 (1978).
24. W. Demtroder ["]Laser Spectroscopy: Basic Concepts and Instrumentation. (Springer-Verlag Press, New York, 1982); and
- V. S. Letokhov Nonlinear Laser Chemistry: Multiple-Photon Excitation (Springer-Verlag press, New York, 1983).
25. R.N. Daly, *Rev. Sci. Instrum.* **31**, 264 (1960).
26. P. J. Robinson and K. A. Holbrook, Unimolecular Reactions, (Wiley-Interscience, New York, 1972).
27. R. Remington and H.F. Schaefer III., unpublished results.
28. M. D. Newton and S. Ehrenson, *J. Am. Chem. Soc.* **93**, 4971 (1971).
29. M. D. Newton, *J. Chem. Phys.* **67**, 5535 (1977).
30. A. Potier, J. M. Leclercq, and M. Allavena, *J. Phys. Chem.* **88**, 125 (1984).
31. G. V. Yuhnevich, E. G. Kokganova, A. I. Pavlyuchko, and V. V. Volkov, *J. Mol. Struct.* **122**, 1 (1985).
32. M. Okumura, L. I-C. Yeh, J. D. Meyers and Y. T. Lee, *J. Chem. Phys.* **85**, 2328 (1986).
33. L. I-C. Yeh, M. Okumura, J. D. Myers, J. M. Price, and Y. T. Lee, *J. Chem. Phys.* **91**(12), 7319, (1989).
34. C.I. Ratcliffe and D.E. Irish, *Water Science Reviews* 2, F. Franks, ed. (Cambridge University Press, Cambridge, 1986); *Water Science Reviews* 3, 1988.
35. S. Scheiner and L.B. Harding, *J. Am. Chem. Soc.* **103**, 2169 (1981).

36. K. Hirao, T. Fujikawa, H. Konishi, and S. Yamabe, *Chem. Phys. Lett.* **104**, 184 (1984).
37. W. S. Benedict, E. K. Plyler, and E. D. Tidwell, *J. Chem. Phys.* **32**, 32 (1960).
38. G. Herzberg, *Infrared and Raman Spectroscopy* (Van Nostrand, Princeton, 1945).
39. W.F. Bennett and C.F. Meyer, *Phys. Rev.* **32**, 888 (1928).
40. N.L. Owen, "Studies of Internal Rotation by Microwave Spectroscopy" in *Internal Rotation In Molecules* W.J. Orville-Thomas, ed. (Wiley Interscience, New York, 1974).
41. P.R. Bunker and H.C. Longuet-Higgins, *Proc. Roy. Soc. (London)*, Ser. A **280**, 340 (1964).
42. D. Papousek, *J. Mol. Spectr.* **28**, 161 (1968).
43. W.B. Olson and D. Papousek, *J. Mol. Spectr.* **37**, 527 (1971).
44. I. M. Mills and H.W. Thompson, *Proc. Roy. Soc. (London)*, Ser. A **226**, 306 (1954).
45. J. Nakagawa, M. Hayashi, Y. Endo, S. Saito and E. Hirota, *J. Chem. Phys.* **80**, 5922 (1984).
46. G.T. Fraser, K.R. Leopold, and W. Klemperer, *J. Chem. Phys.* **81**, 2577 (1984).
47. M. Okumura, L. I-C Yeh, and Y.T. Lee, *J. Chem. Phys.* **83**, 3705, (1985).
48. M. Okumura L.I-C Yeh, J.D. Meyers, and Y.T. Lee, *J. Chem. Phys.* **85**, 2328, (1986).
49. G.C. Pimentel, M.O. Bulanin, and M. Van Theil, *J. Chem. Phys.* **36**, 500 (1962).
50. G. Herzberg, *Infrared and Raman Spectra of Polyatomic Molecules* (D. Van Nostrand, New York, 1945) p. 231, 307.
51. G.C. Pimentel, M.O. Bulanin and M. Van Thiel, *J. Chem. Phys.* **36**, (1962).
52. J.F. Bertran, *J. Mol. Str.* **95**, 9 (1982); J. Corset and J. Lascombe, *J. Chem. Phys.* **64**, 665 (1967).
53. M. Vernon, Ph.D. Thesis, University of California, Berkeley, 1982.

54. D.D. Nelson, Jr., G.T. Fraser, and W. Klemperer, J. Chem. Phys. **83**, 6201 (1985).

TABLE I. Molecular Constants^a for NH₄⁺ and NH₃:

NH ₄ ⁺ (T _d Symmetry)	NH ₃ (C _{3v} Symmetry)
ν_1 : 3270 ± 25 ^b	ν_1 : 3336.21 ^c
ν_2 : 1669 ^d	ν_2 : 950 ^e
ν_3 : 3343.28 ^f	ν_3 : 3444 ^e
ν_4 : 1447.22 ^g	ν_4 : 1627 ^e
	$2\nu_4^o$: 3216.71 ^c
	$2\nu_2^o$: 3240.45 ^c
A=B=C: 5.9293 ± 0.0002 ^f	B=C: 9.941 ^h
ζ_3 : 0.0604 ^f	A: 6.30 ₉ ^h
	ζ_3 : 0.06 ^h

^aUnits are cm⁻¹ for all constants except ζ_3 , which is dimensionless.

^bP. Botschwina, J. Chem. Phys. **87**, 1453 (1987), scaled ab initio value.

^cW.S. Benedict, E.K. Plyler and E.D. Tidwell, J. Chem. Phys. **32**, 32 (1960).

^dD.J. DeFrees and A.D. McLean, J. Chem. Phys. **82**, 333 (1985), scaled ab initio value.

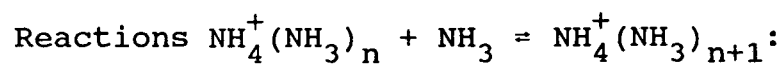
^eT. Shimanouchi, Tables of Molecular Vibrational Frequencies, U.S. Dept. of Commerce, Natl. Stand. Ref. Data Ser. Natl. Bur. Stand. **39** (U.S. GPO, Washington, D.C., 1972).

^fReference 14.

^gM. Polak, M. Gruebele, B.W. DeKock and R.J. Saykally, Mol. Phys. **66**, 1193 (1989).

^hSee Ref. 38, p. 437.

TABLE II. Thermodynamic Data for Gas Phase Clustering



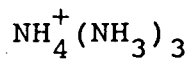
Values are in kcals/mol.

n, n+1	ΔG_{298}° (ref. a)	ΔH_{298}° (ref. a)	(ref. b)	(ref. c)	ΔH_0° (ref. d)
0, 1	-17.5	-27	-25.4	-21.5	-13.8
1, 2		-17	-17.3	-16.2	- 6.4
2, 3	- 6.4	-16.5	-17.3	-13.5	
3, 4	- 3.8	-14.5	-14.2	-11.7	
4, 5	- 0.2	- 7.5	-11.8	- 7.0	

- a. S. K. Searles and P. Kebarle, *J. Phys. Chem.*, **72**, 742 (1968).
 b. I. N. Tang and A. W. Castleman Jr., *J. Chem. Phys.* **62**, 4576 (1972).
 c. M. R. Arshadi, J. H. Futrell, *J. Phys. Chem.* **78**, 1482 (1974).
 d. S. T. Ceyer, P. W. Tiedemann, B. H. Mahan, and Y. T. Lee, *J. Chem. Phys.*, **70**, 14 (1979).

TABLE III. Vibrational frequencies for the ammoniated ammonium ions. Experimental frequencies from this work were found using the IRMPD technique. Units are in cm^{-1} .

This Work	Previous Work ^a	Assignment	
$\text{NH}_4^+(\text{NH}_3)$			
3376.6		$\left. \begin{array}{l} P_{Q_2} \\ PQ_1 \\ R_{Q_0} \\ R_{Q_1} \\ R_{Q_2} \end{array} \right\} \text{NH}_3 \nu_3 \text{ asym stretch}$	
3377.4			
3387.0			
3387.8			
3397.4	3420 (shoulder)		
3398.2			
3409.2			
3419.5			
3392.0			$P_{R_1}(J)?$ (see text)
3402.1			$R_{R_0}(J)?$ (see text)
3412.4		$R_{R_1}(J)?$ (see text)	
$\text{NH}_4^+(\text{NH}_3)_2$			
3392.0		P_{Q_2} of $\text{NH}_3 \nu_3$ overlapped with NH_4^+ free N-H asym str	
3395.4	3360	NH_4^+ free N-H asym str	
3401.9		$\left. \begin{array}{l} P_{Q_1} \\ R_{Q_0} \\ R_{Q_1} \end{array} \right\} \text{NH}_3 \nu_3 \text{ asym stretch}$	
3413.7			
3425.8			
3426.8			



2615

 $\text{NH}_4^+ \nu_1' ({}^3_0\text{N-H}_{\text{sstr}}^{\text{bd}})?$

2660

 $\text{NH}_4^+ \nu_1' ({}^3_0\text{N-H}_{\text{sstr}}^{\text{bd}})$ or

 $\nu_3'' ({}^3_0\text{N-H}_{\text{astr}}^{\text{bd}})$

2692

" "

3374.1

3365

 NH_4^+ free N-H Str

 $\nu_3' ({}^1_0\text{N-H}_{\text{astr}}^{\text{fr}})$

3390.8

 $\left. \begin{array}{l} \text{P}_{\text{Q}_2} \\ \text{P}_{\text{Q}_1} \end{array} \right\}$

3393.1

3404.2

 $\left. \begin{array}{l} \text{R}_{\text{Q}_0} \\ \text{R}_{\text{Q}_1} \end{array} \right\}$

3404.9

3416.8

 $\text{NH}_3 \nu_3$
 asym stretch

3429.0

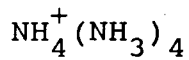
 $\left. \begin{array}{l} \text{R}_{\text{Q}_1} \\ \text{R}_{\text{Q}_2} \end{array} \right\}$

3429.9

3439.6

 $\left. \begin{array}{l} \text{R}_{\text{Q}_2} \\ \text{R}_{\text{Q}_3} \end{array} \right\}$

3452.3



2865

2867

 NH_4^+ asym stretch

 $\nu_3 ({}^4_0\text{N-H}_{\text{astr}}^{\text{bd}})$

3095

3087

 NH_4^+ Bend

 $2\nu_4 ({}^4_0\text{N-H}_{\text{bend}}^{\text{bd}})$

3383.0

 $\left. \begin{array}{l} \text{P}_{\text{Q}_3} \\ \text{P}_{\text{Q}_2} \end{array} \right\}$

3384.3

3393.5

 $\left. \begin{array}{l} \text{P}_{\text{Q}_1} \\ \text{R}_{\text{Q}_0} \end{array} \right\}$

3394.2

3407.8

 $\left. \begin{array}{l} \text{R}_{\text{Q}_1} \\ \text{R}_{\text{Q}_2} \end{array} \right\}$

3408.4

 $\text{NH}_3 \nu_3$
 asym stretch

3420.5

 $\left. \begin{array}{l} \text{R}_{\text{Q}_0} \\ \text{R}_{\text{Q}_1} \end{array} \right\}$

3432.8

3433.3

3443.3
3444.1
3454.9
3456.5

R_{Q_2}
 R_{Q_3}

$\text{NH}_4^+(\text{NH}_3)_5$

2650

$\text{NH}_4^+ \nu_3''$ stretch ($1^0 \text{N-H}_{\text{str}}^{\text{bd, bd}}$)

2880

$\text{NH}_4^+ \nu_3'$ sym stretch ($3^0 \text{N-H}_{\text{sstr}}^{\text{bd}}$)

2910

$\text{NH}_4^+ \nu_1'$ asym stretch ($3^0 \text{N-H}_{\text{astr}}^{\text{bd}}$)

3010 (two peaks)

See text for tentative assignment

3110 (two peaks)

NH_4^+ bend overtone (see text)

3228

Overlap of NH_3 $2\nu_4$ and $1^1 \text{N-H}_{\text{str}}^{\text{bd}}$

3364.4

NH_3 free N-H asym str ($2^1 \text{N-H}_{\text{astr}}^{\text{fr}}$)

3382.7

3383.8

3394.1

3395.2

3407.2

3408.2

P_{Q_3}
 P_{Q_2}
 P_{Q_1}

$1^0 \text{NH}_3 \nu_3$
asym str³

3419.8

3433.0

3443.5

3455.6

3456.3

R_{Q_0}
 R_{Q_1}
 R_{Q_2}
 R_{Q_3}

$\text{NH}_4^+(\text{NH}_3)_6$

2720

$2^0 \text{N-H}_{\text{astr}}^{\text{bd, bd}}$

2910

$2^0 \text{N-H}_{\text{sstr}}^{\text{bd}}$

2950

$2^0 \text{N-H}_{\text{astr}}^{\text{bd}}$

3020

NH_4^+ bend overtone

3228	1°NH_3 H-bonded str ($1^\circ \text{N-H}_{\text{str}}^{\text{bd}}$)
3368.4	1°NH_3 free N-H str ($2^\circ \text{N-H}_{\text{astr}}^{\text{fr}}$)
3398.2	$\left. \begin{array}{l} P_{Q_2} \\ P_{Q_1} \\ R_{Q_0} \\ R_{Q_1} \\ R_{Q_2} \end{array} \right\} 1^\circ \text{NH}_3 \nu_3$ asym str³
3410.8	
3423.7	
3435.7	
3448	
$\text{NH}_4^+(\text{NH}_3)_7$	
2770	$3^\circ \text{N-H}_{\text{astr}}^{\text{bd, bd}}$
2870	Combination of above with hydrogen bond stretch
2955	$1^\circ \text{N-H}_{\text{str}}^{\text{bd}}$
3050	NH_4^+ bending overtone
3220	$1^\circ \text{N-H}_{\text{str}}^{\text{bd}}$
3375	$2^\circ \text{N-H}_{\text{astr}}^{\text{fr}}$
3415	Overlap of $3^\circ \text{N-H}_{\text{astr}}^{\text{fr}}$ and $3^\circ \text{N-H}_{\text{astr}}^{\text{fr}}$ (?), unable to assign subbands for $3^\circ \text{N-H}_{\text{astr}}^{\text{fr}}$
$\text{NH}_4^+(\text{NH}_3)_8$	
2820	$4^\circ \text{N-H}_{\text{astr}}^{\text{bd, bd}}$ ($\text{NH}_4^+ \nu_3$)
2910	Combination of above with hydrogen bond stretch?
3050	$4^\circ \text{N-H}_{\text{bend}}^{\text{bd, bd}}$ overtone ($\text{NH}_4^+ 2\nu_4$)
3220	$1^\circ \text{N-H}_{\text{str}}^{\text{bd}}$ for each of four "identical" subunits, possible overlap from $2^\circ \text{NH}_3 2\nu_4$
3300	$2^\circ \text{N-H}_{\text{sstr}}^{\text{fr}}$?
3320	$2^\circ \text{NH}_3 \nu_1$ ($3^\circ \text{N-H}_{\text{str}}^{\text{f}}$) ?

3380

 $2^{\circ}\text{N-H}_{\text{astr}}^{\text{fr}}$

3415

 $2^{\circ}\text{NH}_3 \nu_3 (^3 2^{\circ}\text{N-H}_{\text{astr}}^{\text{fr}})$ $\text{NH}_4^+(\text{NH}_3)_9$

2829

 $\text{NH}_4^+ \nu_3$ asym stretch $\text{NH}_4^+(\text{NH}_3)_{10}$

2841

 $\text{NH}_4^+ \nu_3$ asym stretch

FIGURE CAPTIONS

1. The normal vibrations of tetrahedrally symmetric NH_4^+ . ν_3 and ν_4 are three fold degenerate, while ν_1 and ν_2 are one and two fold degenerate, respectively. Arrows in the figure indicate the direction of motion but are not to scale with the amplitudes. (See ref. 38)
2. Schematic diagram of the ion source, which consists of a corona discharge and supersonic expansion.
3. Schematic diagram of the experimental apparatus.
4. Mass spectra showing the $\text{NH}_4^+(\text{NH}_3)_n$ cluster distribution as a function of ion source conditions. For 4a, the $\text{NH}_3/\text{H}_2/\text{Ne}$ mixture flowed through a liquid nitrogen trap to reduce the NH_3 concentration. The source backing pressure was raised to obtain 4b, and the trap bypassed to obtain 4c. The $\text{NH}_3/\text{H}_2/\text{Ne}$ mixture was $\approx 1:10:100$.
5. Normal modes of NH_3 . Only one linear combination has been shown for the doubly degenerate modes ν_3 and ν_4 . Again, arrows in the figure indicate the direction of motion but are not to scale for the amplitude of the motion. (See ref. 38)
6. Vibrational predissociation spectra of $\text{NH}_4^+(\text{NH}_3)_n$ ($n=1-6$ for 6a-6f, respectively) in the $3370-3470 \text{ cm}^{-1}$ region, showing the internal rotation subbands. 6g is the same region for the $n=8$ cluster which does not show the internal rotation structure. (Due to poor signal to noise, a larger wavelength

increment was used in scan 6g than the scans in 6a-f, but averaging time was increased.) The notation is discussed in the text. Corresponding subbands are connected by solid lines.

7. C_{3v} and D_{3h} equilibrium structures for $N_2H_7^+$. The energies are expected to differ by only a few kcal/mole, with the relative energy ordering uncertain.

8. Simulated and experimental spectrum of $N_2H_7^+$ for D_{3h} equilibrium structure of fig. 7b. The simulation includes only Q branch transitions, since these are expected to dominate the spectrum. While the two traces show similarities, there are substantial differences as well. Rotational constants used in the simulation: $A'=3.20\text{cm}^{-1}$, $A''=3.16\text{cm}^{-1}$, $B'=B''=0.16\text{cm}^{-1}$, $T=30\text{K}$, $\Delta V=-1.0$, $\zeta=0.0$.

9. Vibrational predissociation spectra of $NH_4^+(NH_3)_n$ ($n=3-8$ for 9a-9f, respectively) in the $2600-3500\text{cm}^{-1}$ region. Bands forming clear series in n are connected by dashed lines.

10. Proposed structures for the $n=4,5$ and 8 complexes. The hydrogen bonds are denoted by dashed lines. It is not certain that the hydrogen bonding between 1° and 2° NH_3 is linear.

11a. Plot of the R_{Q_0} bands for the internal rotation structure associated with the 1° NH_3 's antisymmetric stretching transition as a function of cluster size.

11b. Plot of the peak intensity of the antisymmetric stretching band for the ammonium ion core bound only to 1° NH_3 molecules as a function of cluster size. The series shows eventual

convergence as n increases. See text for discussion.

11c. Plot of the peak intensity of the antisymmetric stretching band for the ammonium ion core bound to both 1° and 2° NH_3 molecules as a function of cluster size. Converged values are similar to those observed for solutions of ammonium salts dissolved in liquid ammonia. See text for discussion.

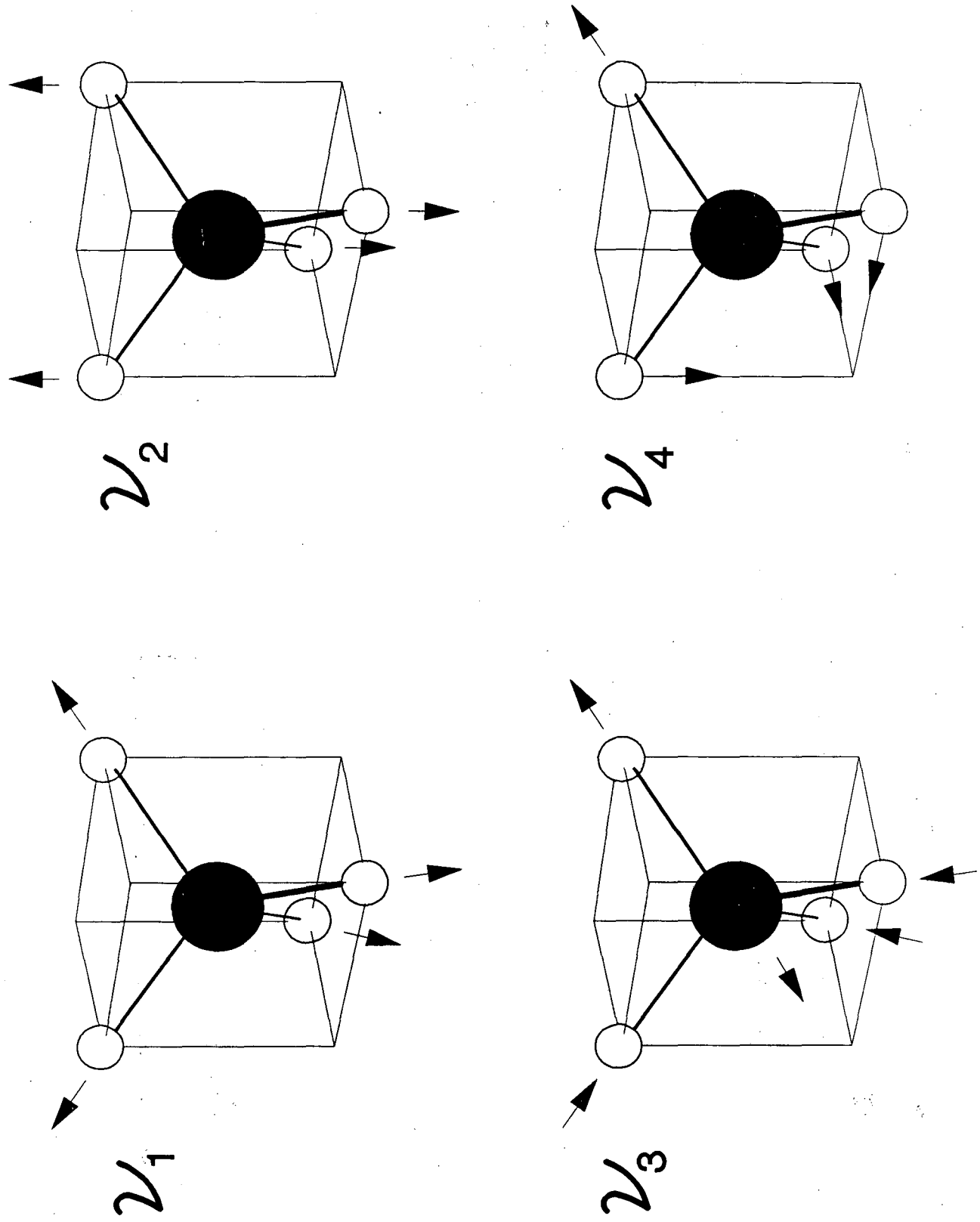


Fig. 1

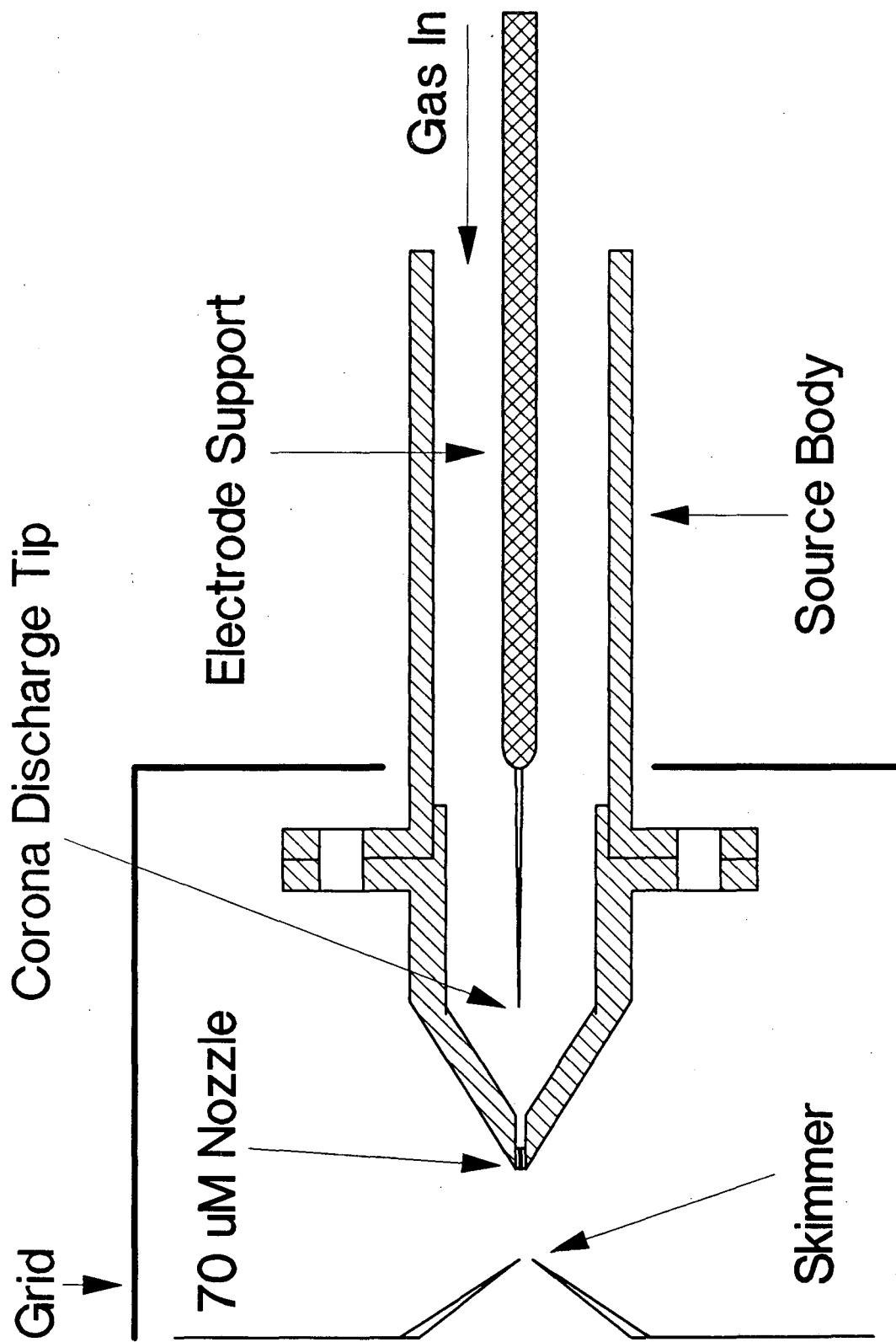


Fig. 2

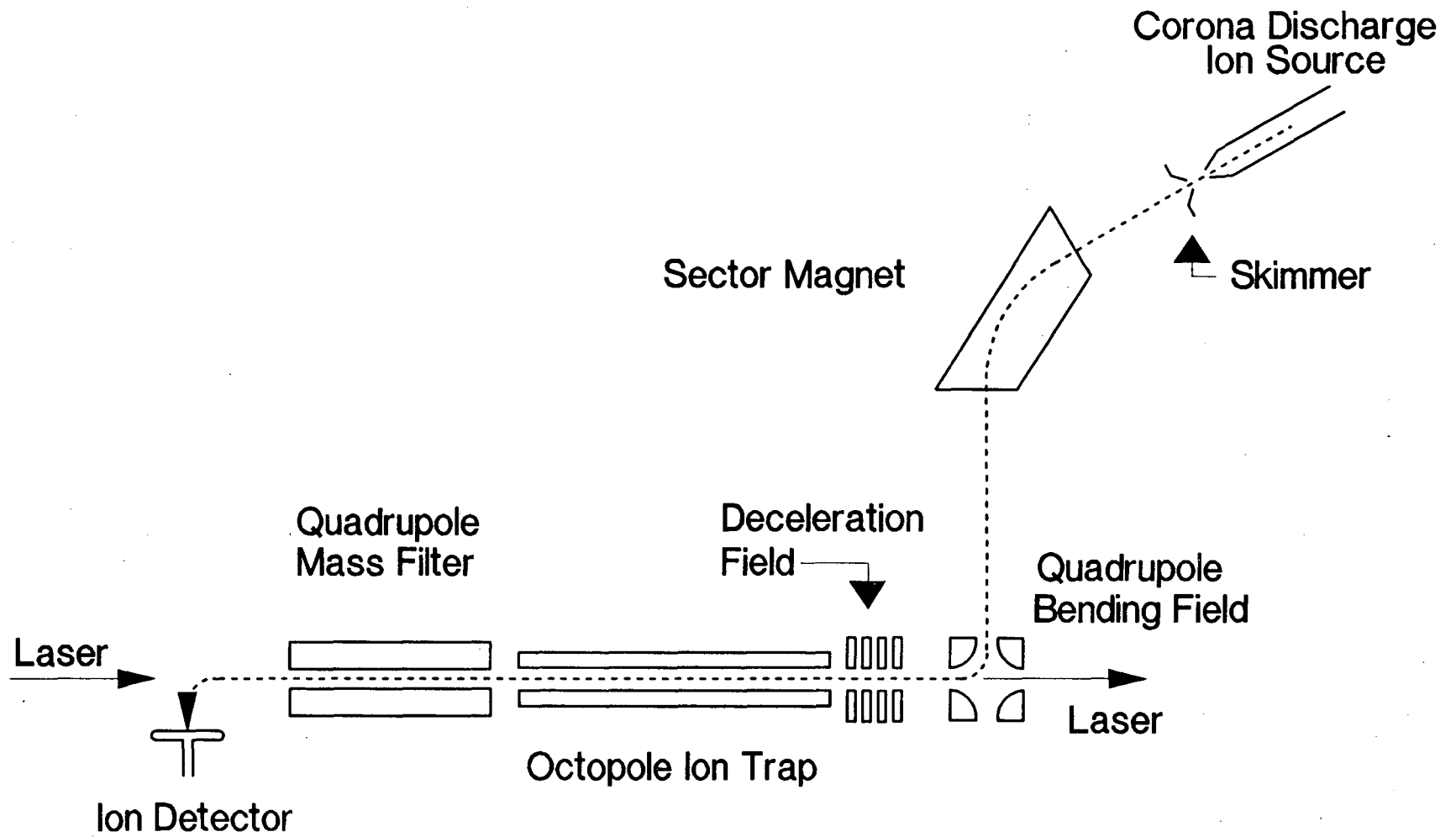
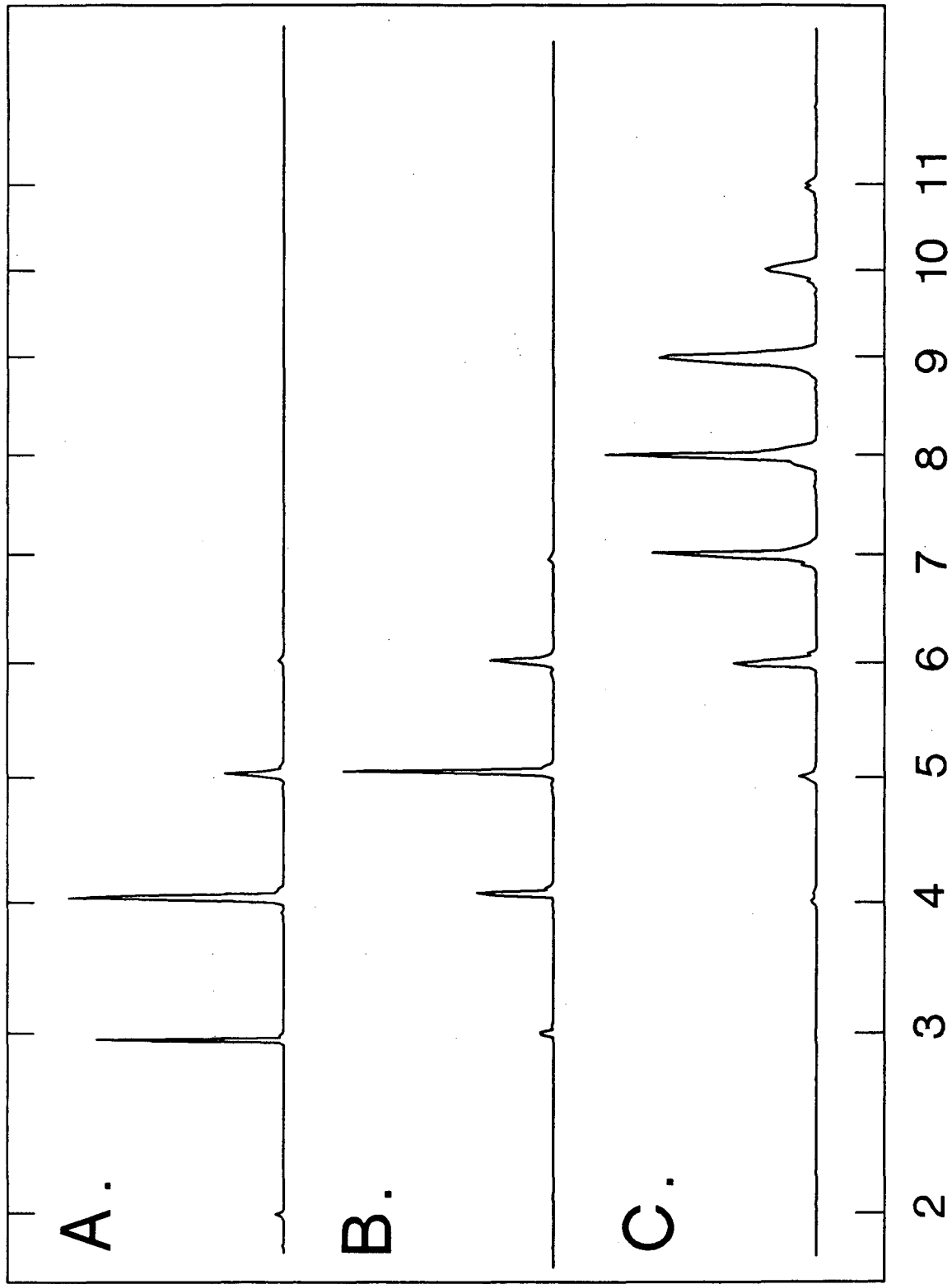


Fig. 3



Number Solvent NH₃'s

Fig. 4

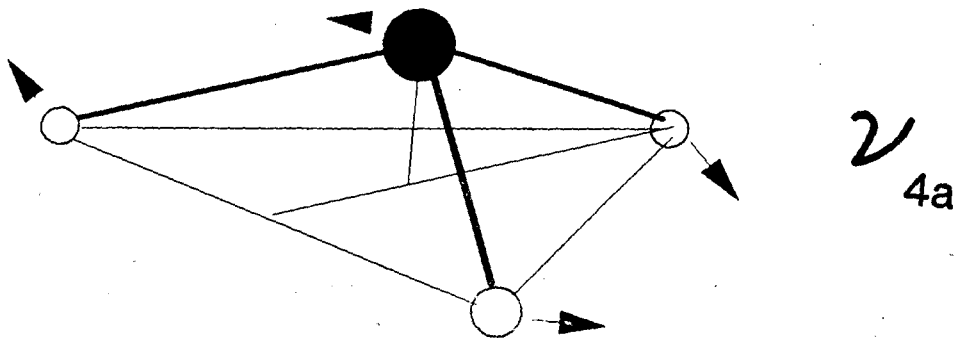
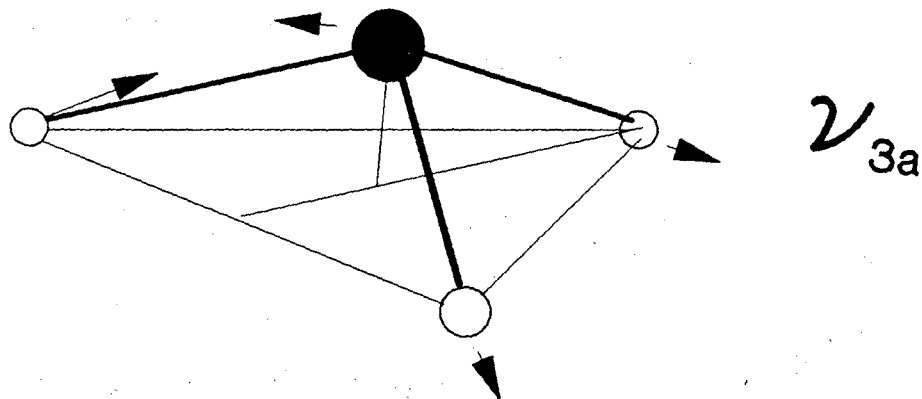
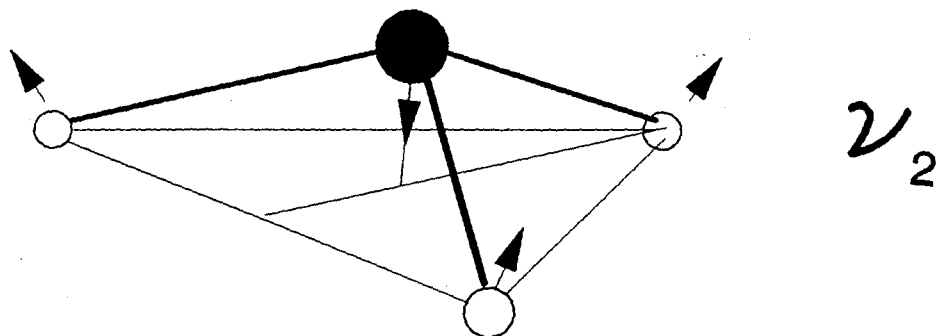
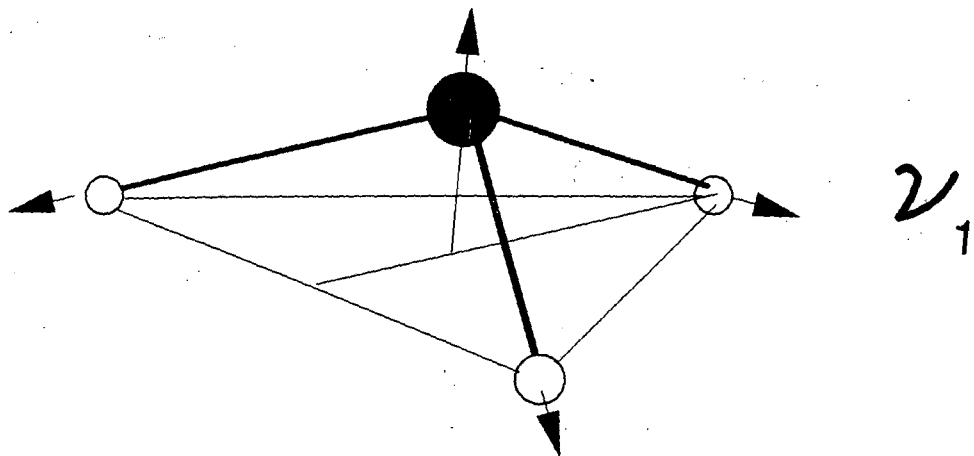


Fig. 5

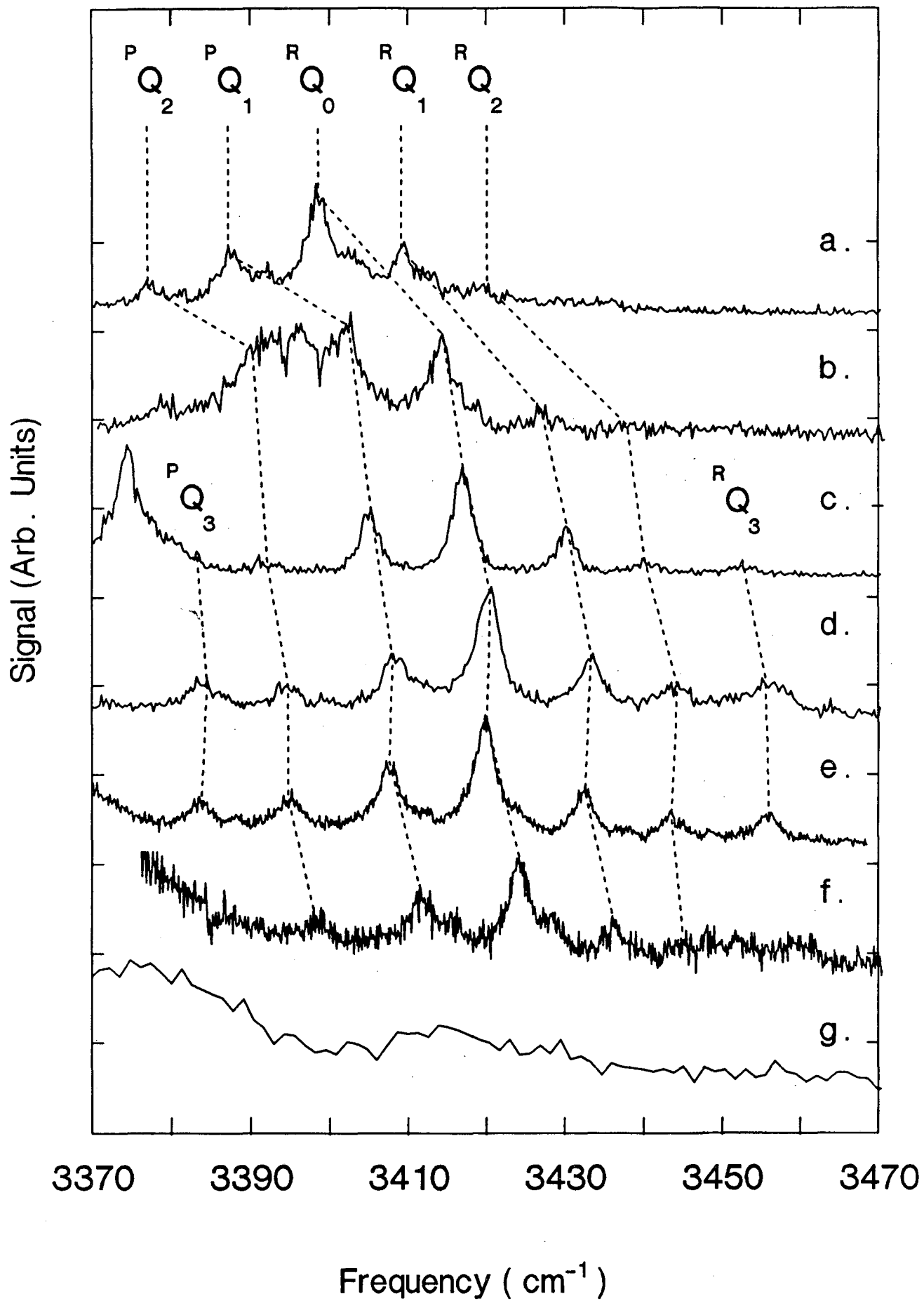


Fig. 6

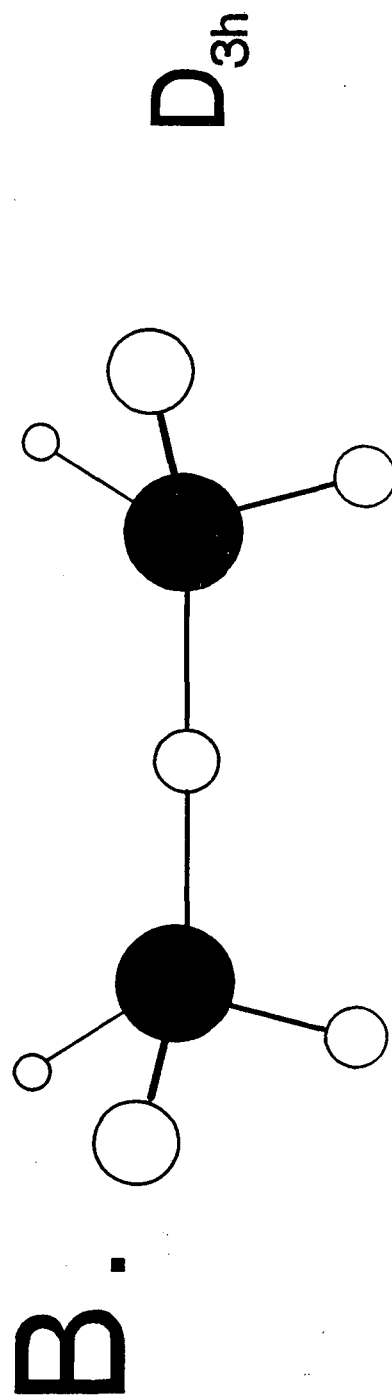
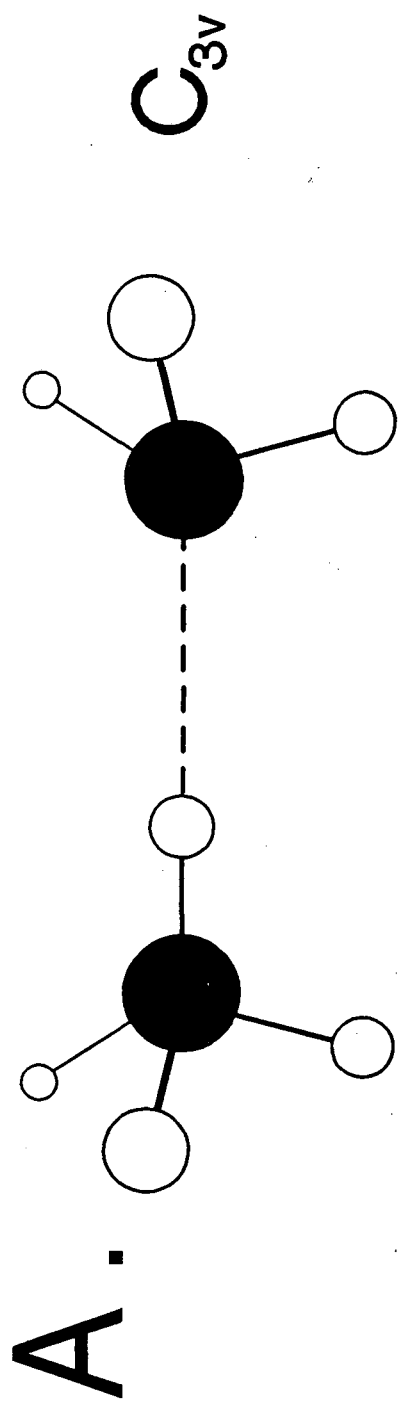


Fig. 7

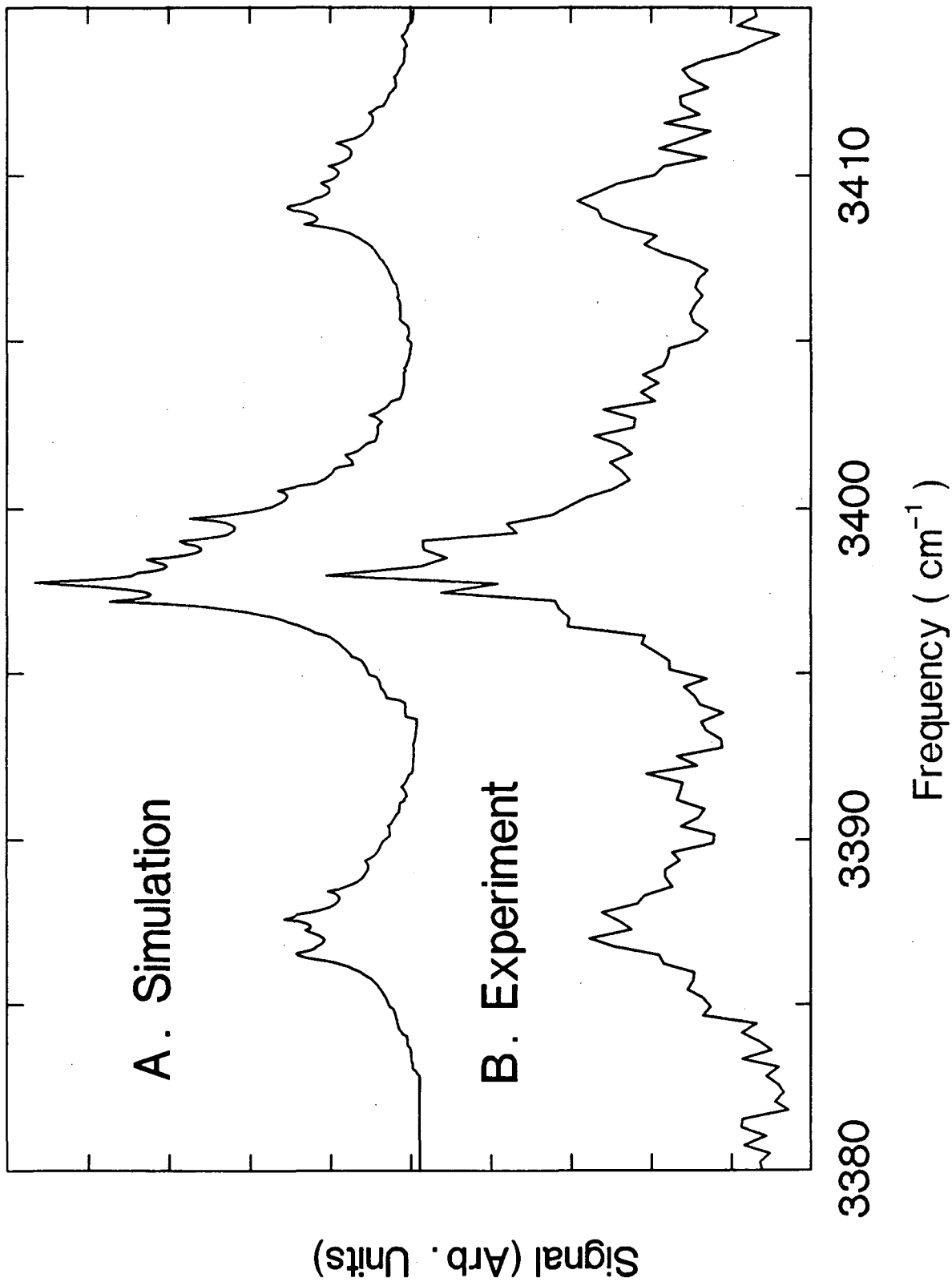


Fig. 8

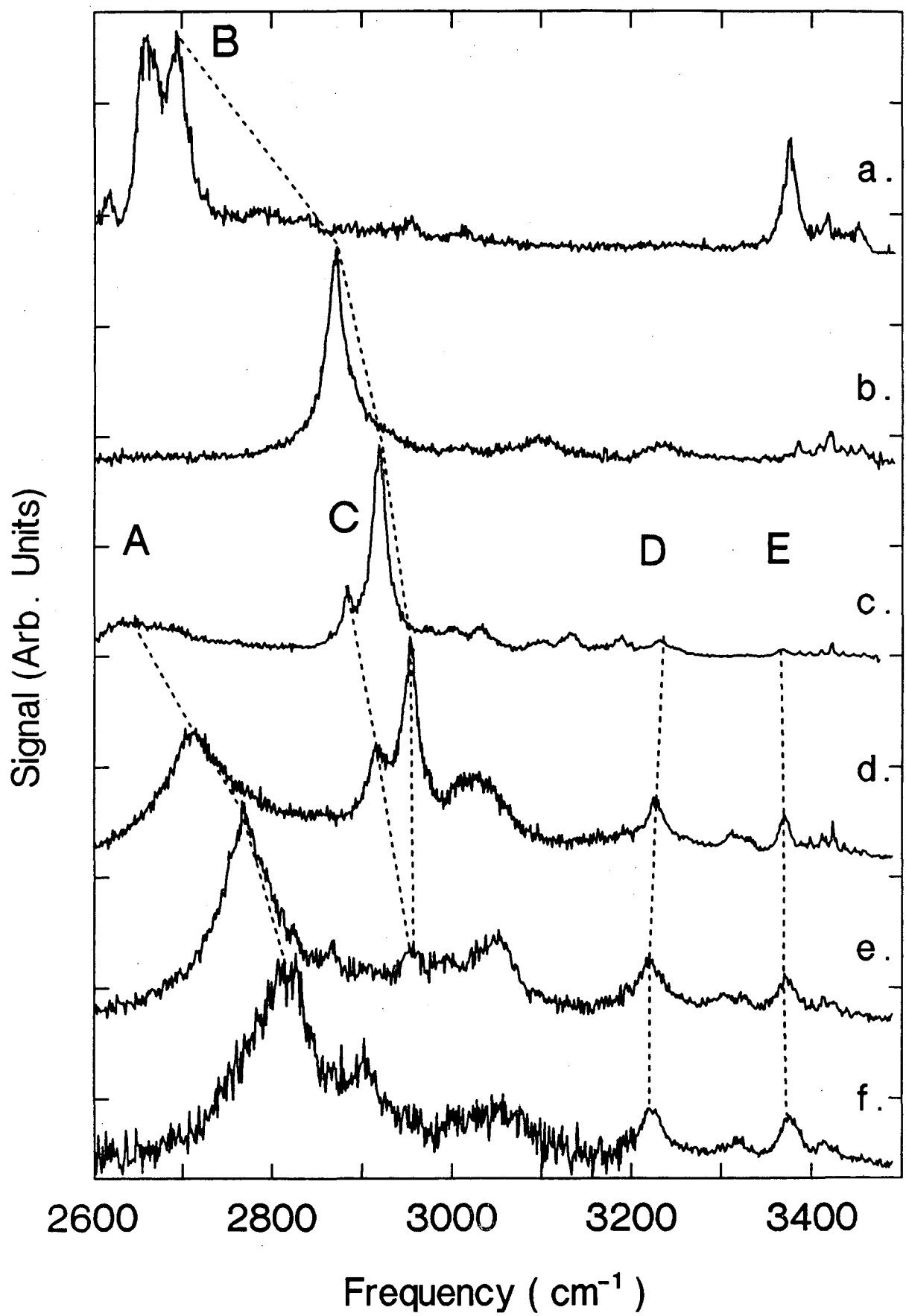
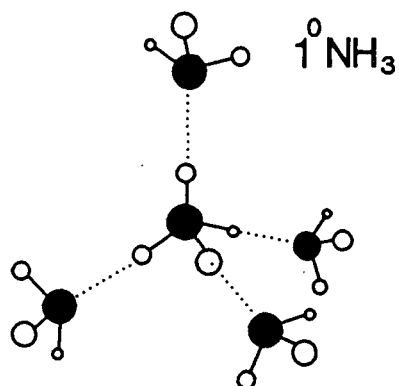
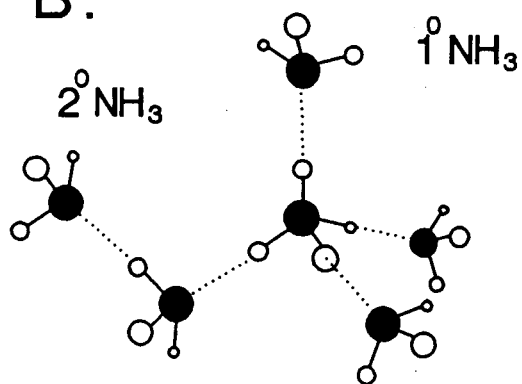


Fig. 9

A.



B.



C.

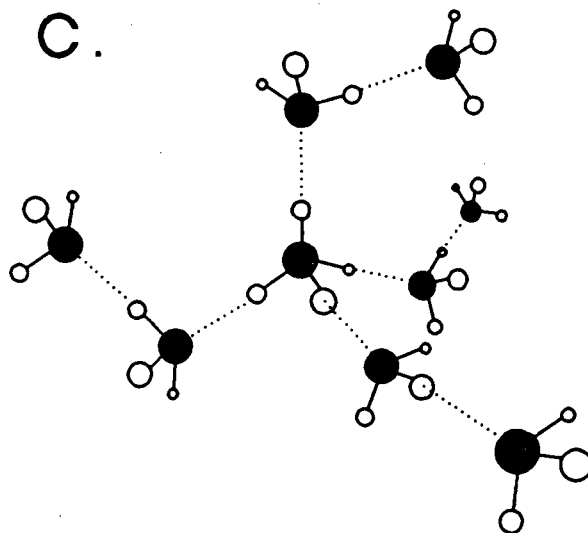


Fig. 10

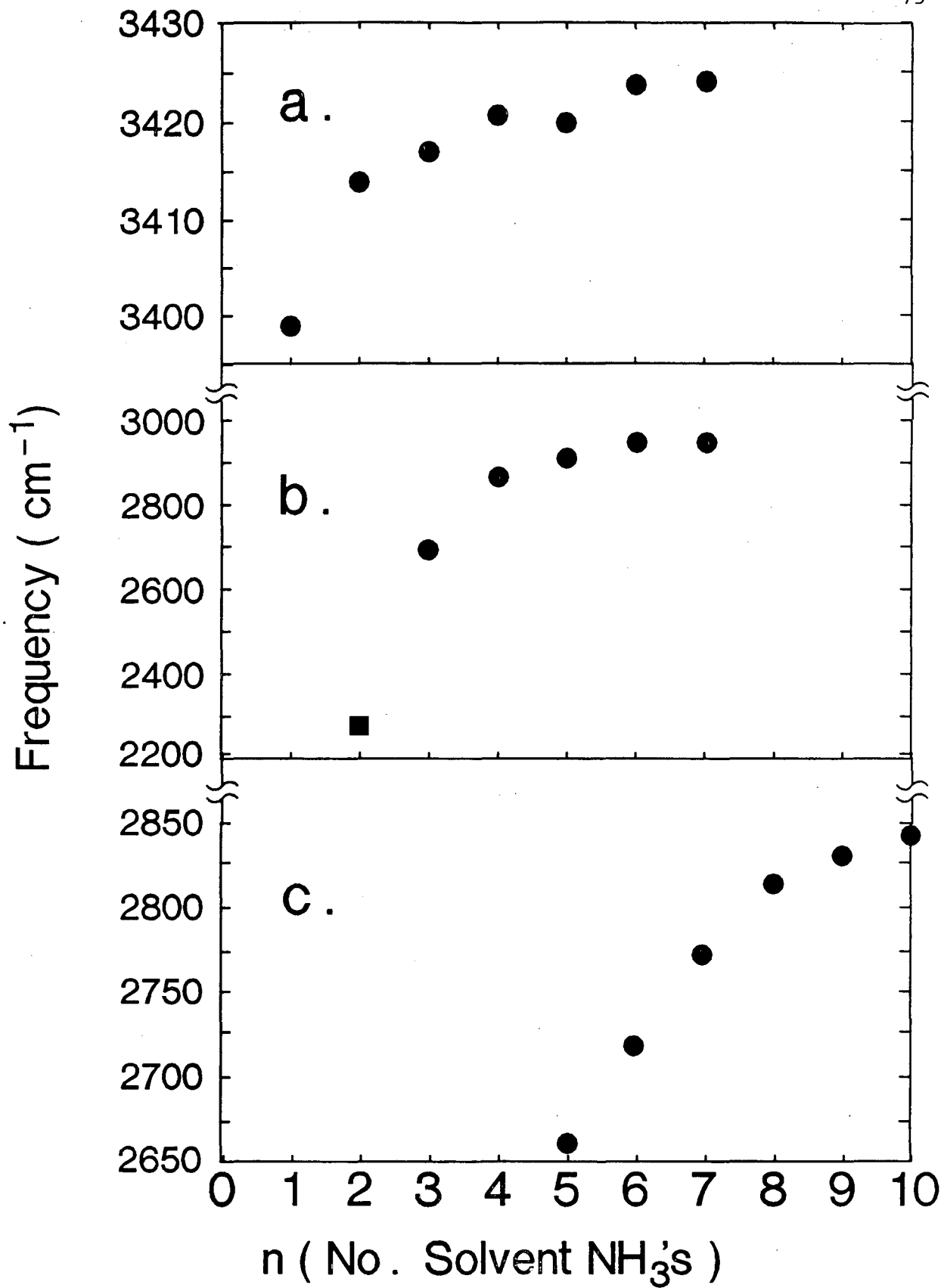


Fig. 11

LAWRENCE BERKELEY LABORATORY
UNIVERSITY OF CALIFORNIA
INFORMATION RESOURCES DEPARTMENT
BERKELEY, CALIFORNIA 94720